PL-TR-94-2147

GLOBAL IONOSPHERIC WEATHER

Dwight T. Decker
Patricia H. Doherty

Boston College
Institute for Space Research
140 Commonwealth Avenue
Chestnut Hill, MA 02167

28 February 1994

Scientific Report No. 1

45

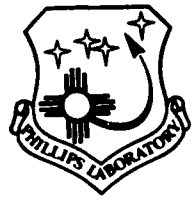

PHILLIPS LABORATORY
Directorate of Geophysics
AIR FORCE MATERIEL COMMAND
HANSCOM AIR FORCE BASE, MA 01731-3010

"This technical report has been reviewed and is approved for publication"

(Signature)
JOHN RETTERER
Contract Manager

(Signature)
FRANK A. MARCOS
Acting Branch Chief

(Signature)
WILLIAM K. VICKERY
Division Director

This report has been reviewed by the ESC Public Affairs Office (PA) and is releasable to the National Technical Information Service (NTIS).

Qualified requestors may obtain additional copies from the Defense Technical Information Center (DTIC). All others should apply to the National Technical Information Service (NTIS).

If your address has changed, if you wish to be removed from the mailing list, or if the addressee is no longer employed by our organization, please notify PL/TSI, 29 Randolph Road, Hanscom AFB, MA 01731-3010. This will assist us in maintaining a current mailing list.

Do not return copies of this report unless contractual obligations or notices on a specific document requires that it be returned.

REPORT DOCUMENTATION PAGE

Form Approved
OMB No. 0704-0188

1. AGENCY USE ONLY (Leave blank)	2. REPORT DATE	3. REPORT TYPE AND DATES COVERED
	28 FEB 1994	Scientific No. 1

4. TITLE AND SUBTITLE

Global Ionospheric Weather

5. FUNDING NUMBERS

C F19628-93-K-0001
PE 63707F
PR 4643
TAGL
WUAA

6. AUTHOR(S)

Dwight T. Decker
Patricia H. Doherty

7. PERFORMING ORGANIZATION NAME(S) AND ADDRESS(ES)

Boston College
Institute for Space Research
140 Commonwealth Avenue
Chestnut Hill MA 02167

8. PERFORMING ORGANIZATION REPORT NUMBER

BC-ISR-94-02

9. SPONSORING/MONITORING AGENCY NAME(S) AND ADDRESS(ES)

Phillips Laboratory
29 Randolph Road
Hanscom AFB MA 01731-3010
Contract Manager: John Retterer/GPIM

10. SPONSORING/MONITORING AGENCY REPORT NUMBER

PL-TR-94-2147

11. SUPPLEMENTARY NOTES

12a. DISTRIBUTION/AVAILABILITY STATEMENT

Approved for public release;
distribution unlimited

12b. DISTRIBUTION CODE

13. ABSTRACT *(Maximum 200 words)*

In the last year, we have studied several issues that are critical for understanding ionospheric weather. Work on global F-region modeling has consisted of testing the Phillips Laboratory Global Theoretical Ionosphere Model. Comparisons with both data and other theoretical models have been successfully conducted and are ongoing. GPS observations, as well as data analysis, are also ongoing. Data have been collected for a study on the limitations in making absolute ionospheric measurements using GPS. Another study on ionospheric variability is the first of its kind using GPS data. The observed seasonal total electron content behavior is consistent with that determined from the Faraday rotation technique. Work on the FAA's Phase 1 Wide Area Differential GPS (WADGPS) Satellite Navigation Testbed Experiment also continues. Initial results indicate that stations using operational WADGPS should be located no greater than 430 km apart. Work comparing our electron-proton-H atom model to both observations and other models has been generally successful. We have successfully modeled the creation of high-latitude large-scale plasma structures using two separate mechanisms (time-varying global convection and meso-scale convection events).

14. SUBJECT TERMS	15. NUMBER OF PAGES
Ionospheric weather, global F-region modeling, total electron content, GPS, TEC, aurora, electron transport, proton-H atom transport, plasma structure, patches	46
	16. PRICE CODE

17. SECURITY CLASSIFICATION OF REPORT	18. SECURITY CLASSIFICATION OF THIS PAGE	19. SECURITY CLASSIFICATION OF ABSTRACT	20. LIMITATION OF ABSTRACT
UNCLASSIFIED	UNCLASSIFIED	UNCLASSIFIED	SAR

TABLE OF CONTENTS

1. INTRODUCTION

The objective of this research is to improve our ability to observe and theoretically model the ionospheric "weather". In this first year, we have studied five issues where we have had the tools and experience to make significant progress. Those issues include: 1) Global F region modeling, 2) GPS observations, 3) Electron backscatter, 4) Proton precipitation, and 5) Modeling high- latitude F-region patches.

2. GLOBAL F REGION MODELING

In this year, we have been testing the Phillips Laboratory Global Theoretical Ionospheric Model (GTIM) in a variety of ways. There have been comparisons with data at both low and midlatitudes. The low-latitude study involved an analysis of a major magnetic storm period in June 1991. The mid-latitude study involved an attempt to model the day-to-day variations of the F2 peak at Wallops Island during the months of December and May 1991. There is also ongoing work comparing GTIM to theoretical models as part of the PRIMO (Problems Related to Ionospheric Modeling and Observations) workshop that has been held at the last three annual CEDAR meetings. Finally, near the end of this first year, we have participated in preparations for the Phillips Laboratory Low-Latitude Ionospheric Tomography Campaign.

2.1 June 1991 Storm Analysis

The month of June 1991 was a period affected by major magnetic storm activity. There were six sudden commencement storms observed between June 3rd and the 16th. Total Electron Content (TEC) measurements recorded at three Air Weather Service Stations, Hamilton MA, Kennedy AFB FL and Ramey, Puerto Rico have been analyzed to observe the effects of this storm activity. These TEC values were obtained from continuous measurements of Faraday polarization changes of VHF radio signals emitted from geostationary satellites of opportunity.

Figure 1 illustrates the results of this analysis. Diurnal curves from each station are plotted for June 8th through the 13th. On June 8th, a sudden commencement storm occurred at 1500 UT (1100 LT for these 3 stations). All three stations responded to this activity with an immediate sharp rise in TEC followed by major depletions for the next two days. Continued geomagnetic disturbances resulted in very unusual, but remarkably similar, observations at Ramey and Kennedy through the 13th of June. Observations at Hamilton were also severely disturbed.

From this analysis, we conclude that the severity of the geomagnetic activity resulted in the appearance of equatorial electrodynamic effects as far north as Florida.

These measurements coincided with model results using the low-latitude portion of GTIM. GTIM is a time-dependent, theoretical model which solves the ion continuity equation for the O^+ concentration through production, loss, and transport of ionization. Observed vertical drift velocities measured at the Jicamarca, Peru incoherent scatter radar facility during the storm were incorporated into the model to calculate electron density profiles as a function of dip latitude and local time. In Figure 2, we illustrate the results of the model by showing contours of Nmax (the F_2 peak density) as a function of dip latitude and local time. Here, the results reveal a strong poleward shift of the equatorial anomaly to as far north as 28 degrees dip latitude. In order to make detailed day-to-day comparisons with data, we plan in the next years to modify GTIM to accept more than 24 hours of drift

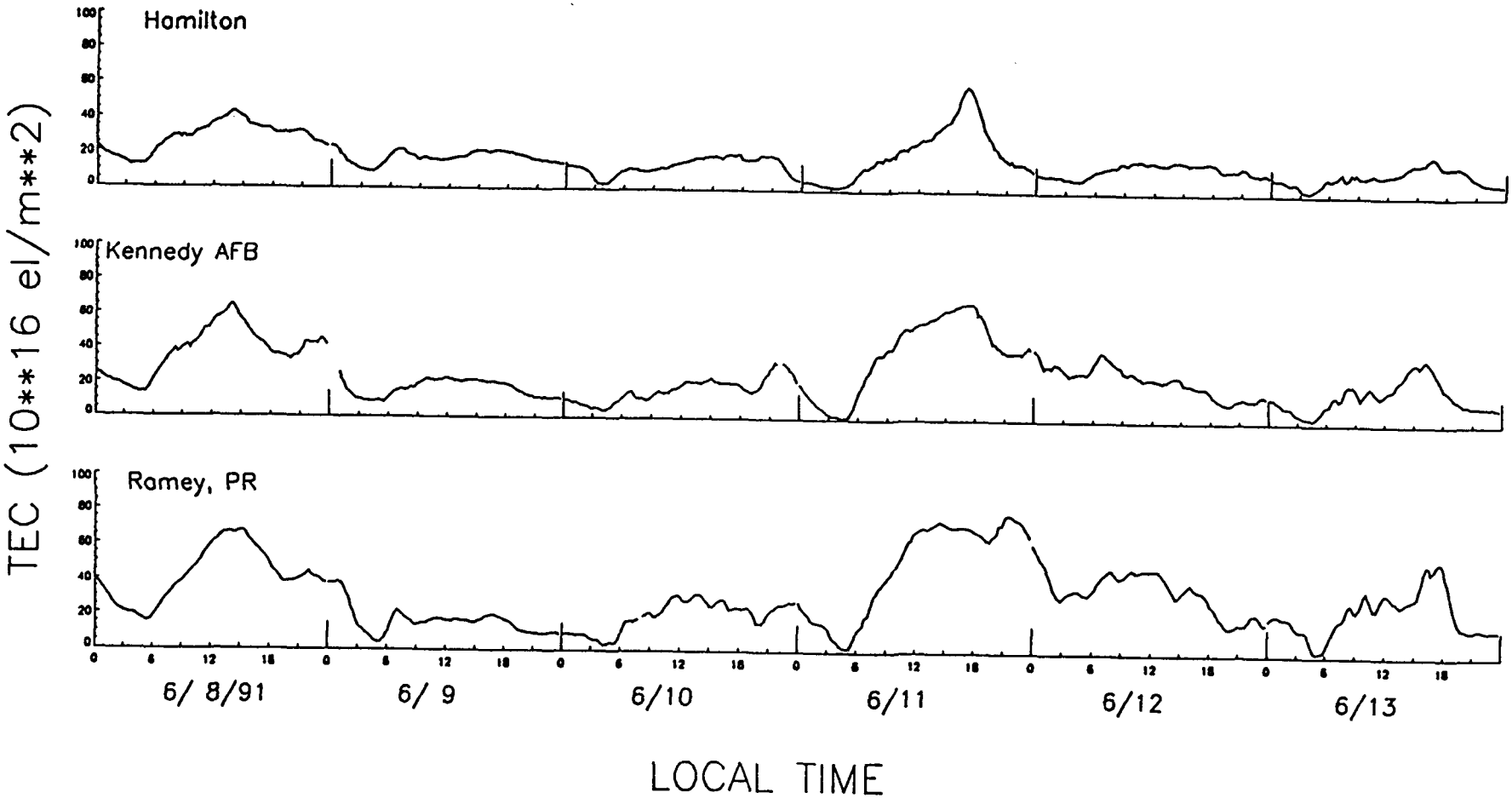
Hamilton
Kennedy AFB
Ramey, PR
TEC (10**16 el/m**2)
6/ 8/91
6/ 9
6/10
6/11
6/12
6/13
LOCAL TIME

Figure 1

AMERICAN SECTOR - JUNE 13, 1991 - DISTURBED CONDITIONS

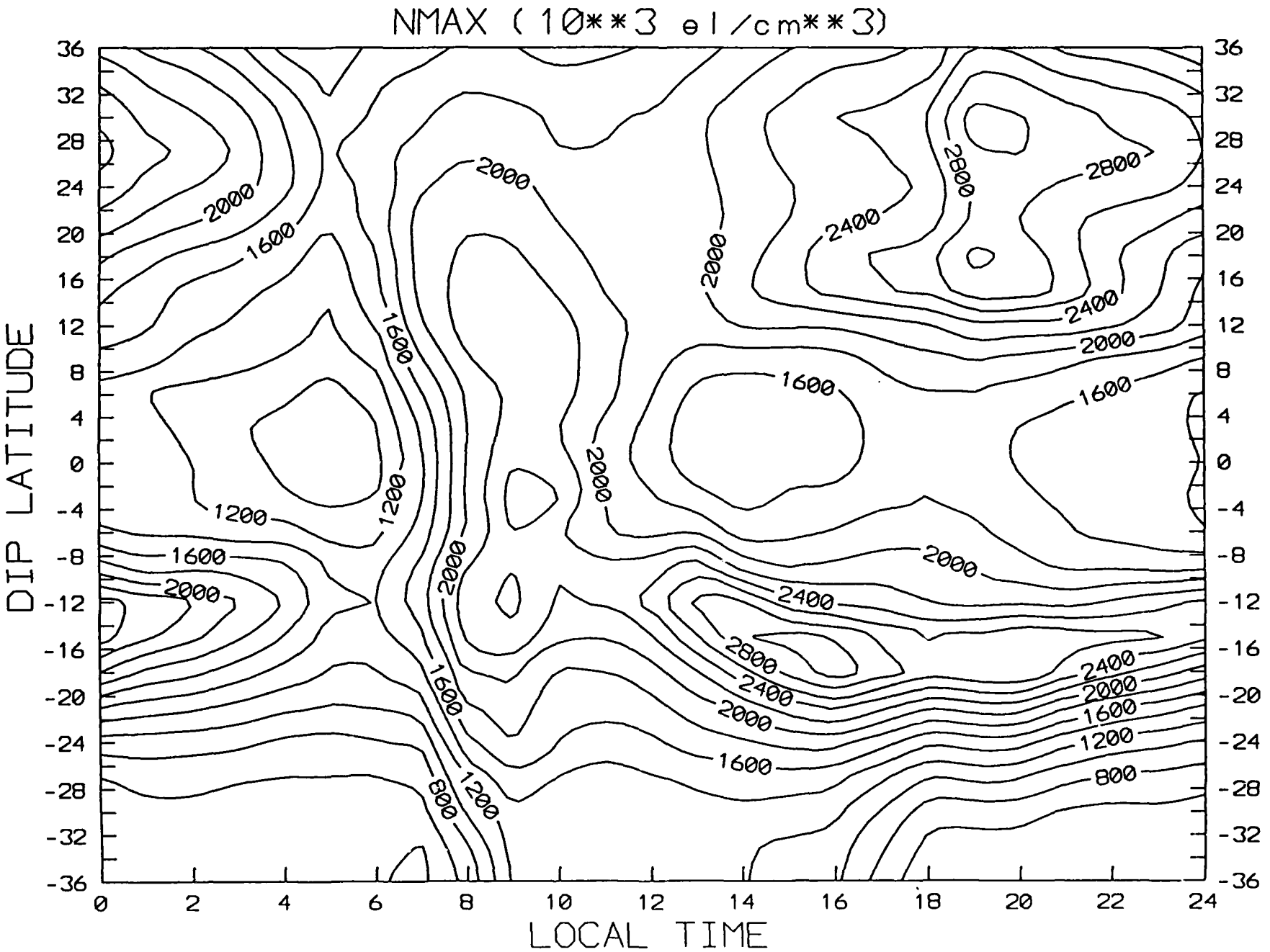

Figure 2

data. This will allow us to simulate an entire period of pre-storm, storm, and post-storm conditions.

2.2 Day-to-Day Comparison of Calculated and Observed Electron Densities at Midlatitudes

Over the last few years, there has been an increasing effort to validate various theoretical models of the earth's ionosphere. In the work done to date, the focus has been almost exclusively on comparisons between a calculation of a 24-hour day using typical or average inputs with either monthly means of observations or data from a "typical" quiet day. But there is growing interest on how well the day-to-day "weather" of the ionosphere can be modeled. With that in mind, we have simulated the day-to-day variations for May and December 1990 at Wallops Island, Virginia.

Our initial goal was to simply see how good or bad a job GTIM does at simulating the day-to-day variability when the model is driven by statistical or empirical geophysical inputs. A follow-on goal was to see how much of any discrepancy between data and theory can be understood in terms of uncertainty in the geophysical inputs. The data we used were the hourly F_2 peak parameters from digisonde measurements made at Wallops Island. GTIM is a one species F-region model that solves the ion continuity and momentum equations. In such a model, it is the day-to-day variation in the required geophysical inputs that causes a day-to-day variation in the model output. This variation in the geophysical inputs is determined by the variability in the F10.7 cm solar flux and the daily magnetic index Ap.

Of all the required geophysical inputs, it is the neutral wind that we suspect is our greatest source of day-to-day variability. Thus, we have simulated the entire months of December and May using three different neutral wind models. The first simulation used HWM-87 and the second used the VSH wind model. The third simulation used the approach of treating the wind as a free parameter and requiring that the model reproduce the observed hmF_2. In Figure 3, we show for the first twelve days of December, 1990 the observed NmF_2 compared to the results from the three simulations. The solid curve is the data, the long dashed curve is the HWM-87 simulation, the middle dashed curve the VSH results, and the shortest dashed curve is from fitting to hmF_2. We see that the HWM-87 does the best, though all three simulations reproduce the gross features of the diurnal behavior. None of the simulations seems to follow the day-to-day variability especially around, and just before, noon. The fact that none of these simulations seems to follow what day-to-day variability there is leads us to suspect that for this month, we cannot understand that variability simply in terms of uncertainties in the neutral wind.

Turning to May, we see dramatically different results. In Figure 4, we show for the first twelve days of May 1990 the observed NmF_2 (solid curve) compared to a simulation using HWM-87 (dashed curve). We see that in both the data and the theory, there is much less diurnal variation than in December. However, the model results are obviously much too large. On some of the quieter days (day 2 and days 5-8), the data and model are in closer agreement, but on magnetically active days such as days 10 and 11, the model has major difficulties. On all days, we see that the model maintains NmF_2 right through until after midnight, whereas on several of the days, the observations show a definite decrease in NmF_2 throughout the pre-midnight period. In looking at the effects of different wind models, we find that the VSH model makes little difference. The results of fitting to hmF_2 are shown in Figure 5, and while on certain days this procedure does produce a decay of NmF_2 in the pre-midnight period, there are days in which the model still has severe problems. What we believe is that the empirical geophysical inputs are simply inadequate during magnetically active periods. In particular, the problem is not

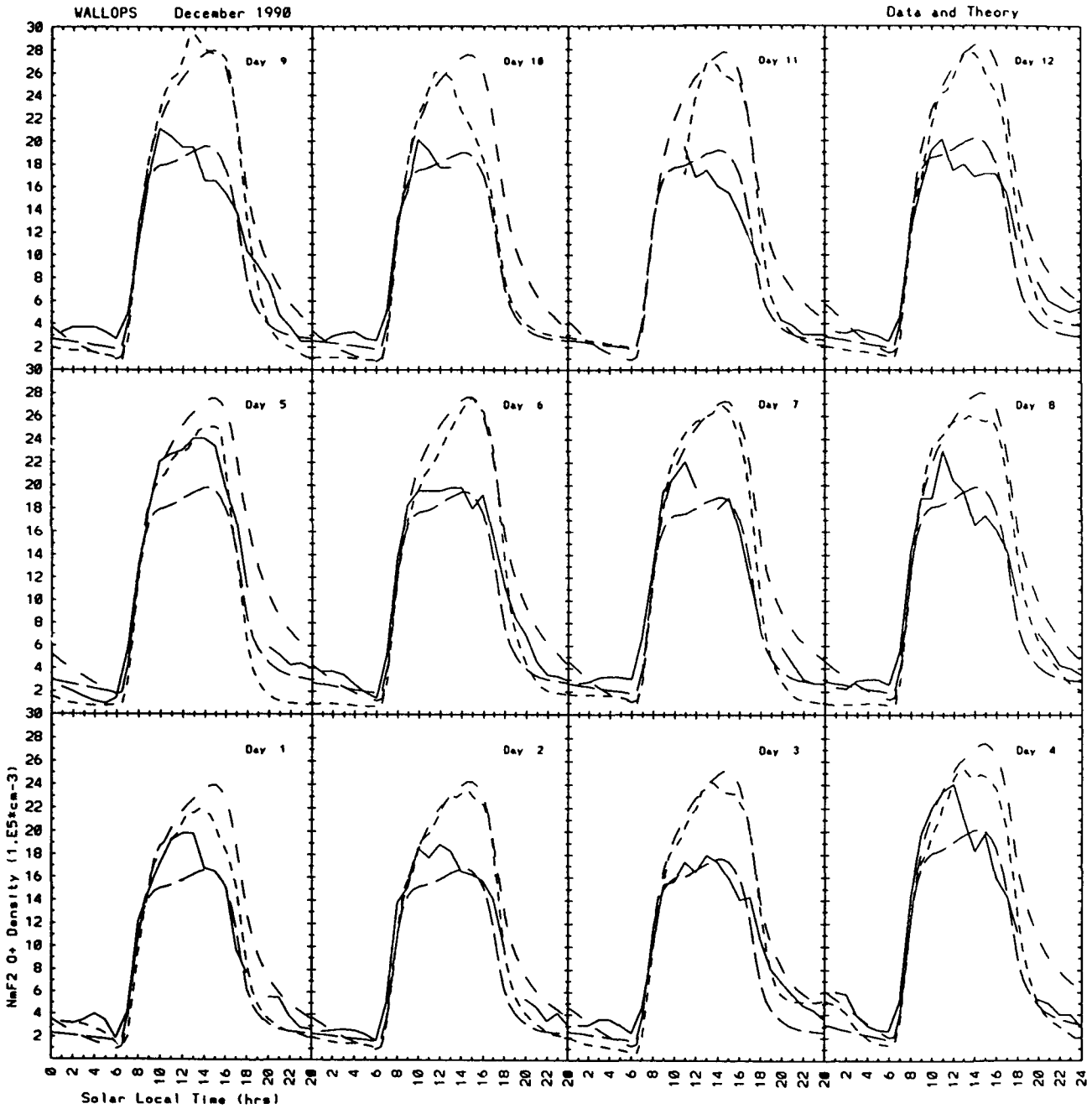
WALLOPS December 1990
Data and Theory
Day 9
Day 10
Day 11
Day 12
Day 5
Day 6
Day 7
Day 8
Day 1
Day 2
Day 3
Day 4
NmF2 O+ Density (1.E5*cm-3)
Solar Local Time (hrs)

Figure 3

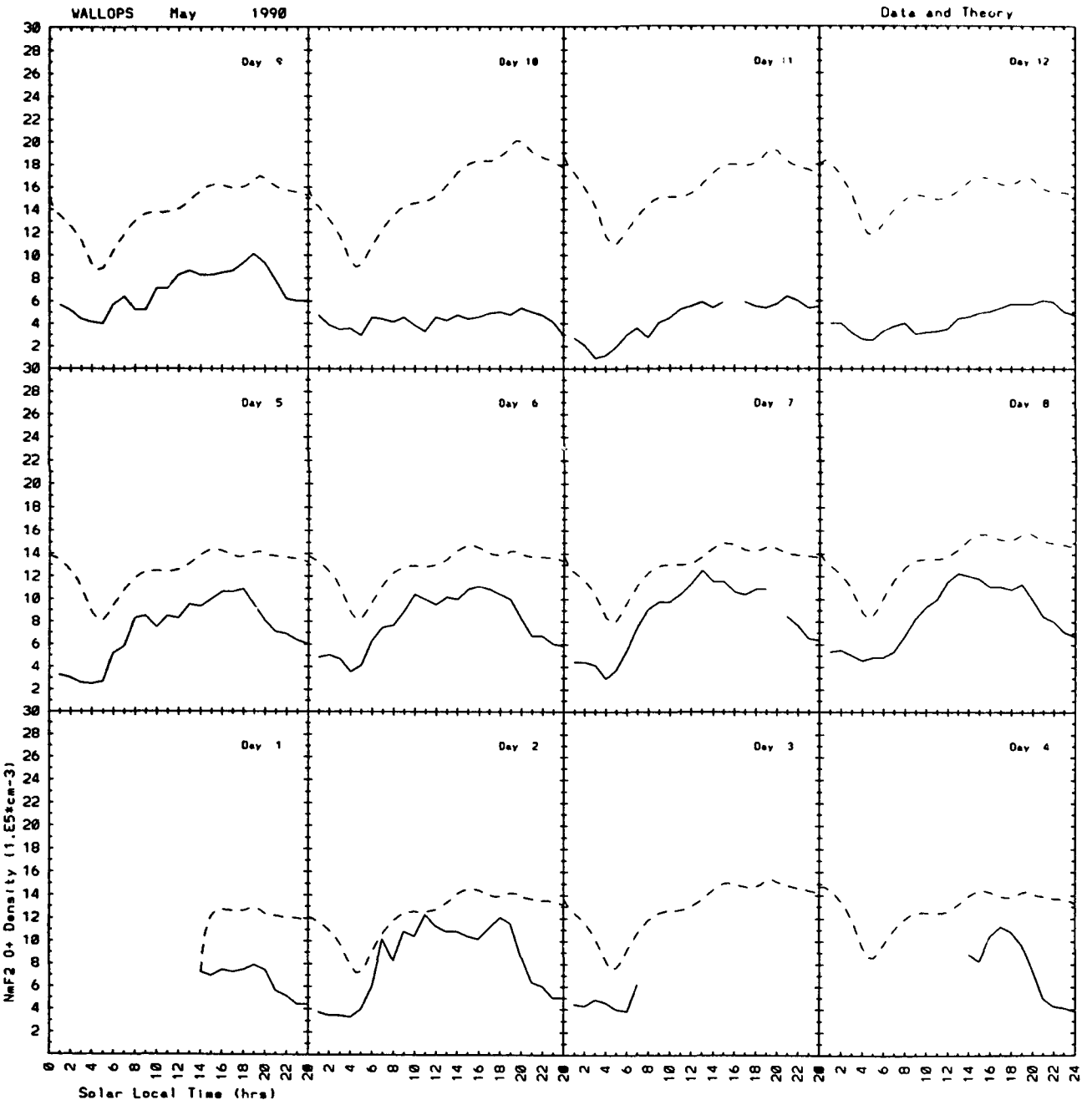
WALLOPS May 1990
Data and Theory
Day 9
Day 10
Day 11
Day 12
Day 5
Day 6
Day 7
Day 8
Day 1
Day 2
Day 3
Day 4
NmF2 O+ Density (1.E5*cm-3)
Solar Local Time (hrs)

Figure 4

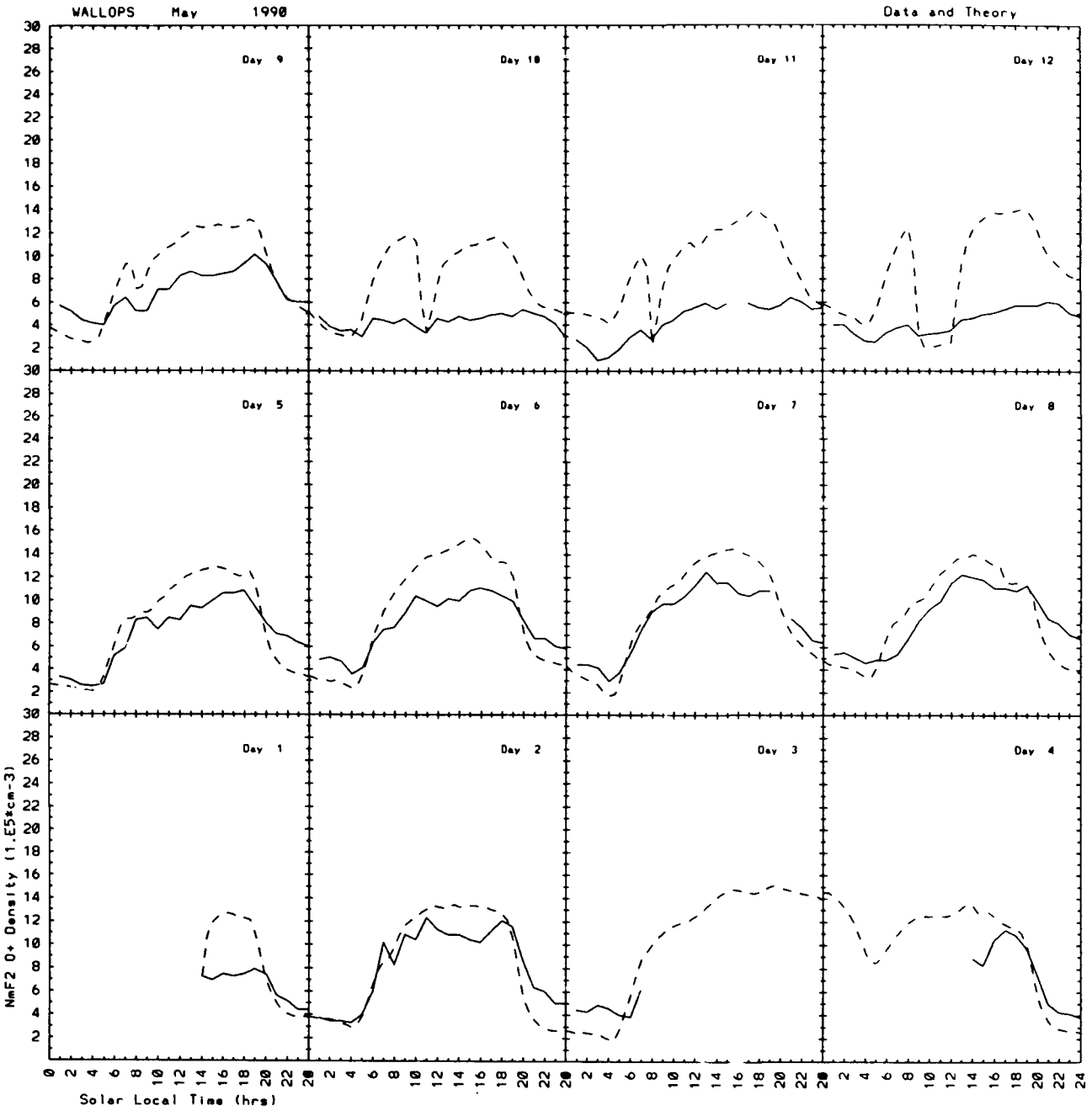
WALLOPS May 1990
Data and Theory
Day 9
Day 10
Day 11
Day 12
Day 5
Day 6
Day 7
Day 8
Day 1
Day 2
Day 3
Day 4
NmF2 O+ Density (1.E5*cm-3)
Solar Local Time (hrs)

Figure 5

confined to just the neutral winds, but mostly likely involves the neutral densities and temperatures as well as possibly the electric fields and plasma temperatures.

Thus, we conclude that while a GTIM driven by statistical or empirical geophysical inputs produces a day-to-day variation, that variation appears to have little to do with the observed variations. For any specific day, we find that the observed monthly median or the GTIM calculated median is likely to be a better predictor than that day's GTIM simulation.

2.3 Theoretical Model Comparisons

As part of our effort in global modeling, we have taken part in the PRIMO workshop that has been held at the last three annual CEDAR meetings. One outcome of those meetings is that the five modeling groups involved are now working on a paper on the "Intercomparison of Physical Models and Observations of the Ionosphere". For that paper, we have begun a careful comparison between our global theoretical ionospheric model (GTIM) and Utah State University's time dependent ionospheric model (TDIM).

As a first step in this study, we chose to compare the model's inputs at three altitudes (125, 250, and 400 km) at each UT hour for a calculation at Millstone Hill under solar maximum winter conditions. Initially, the only large difference was in the source functions at 125 km. Upon examining the entire source profile from GTIM, we found an unreasonably large increase below around 125 km. This increase was the result of round off problems in the implementation of the Chapman function for calculating column densities at large solar zenith angles. This problem has now been solved and we find that all the inputs agree to within a few tens of percents. The next step will be to understand the source of these tens of percents differences.

2.4 Low Latitude Ionospheric Tomography Campaign

Preparations have been made for participation in the Phillips Laboratory Low Latitude Ionospheric Tomography Campaign. From March 28th through April 15th, at least six Magnavox MX1502 Satellite Receiver Systems will be installed and operating in the low-latitude American sector. The purpose of this campaign is to determine the location and magnitude of the equatorial anomaly using the emerging computerized ionospheric tomography technique.

Simultaneous measurements of TEC will be made from a series of stations in the low-latitude American sector. This data set will then be used in a reconstruction of tomographical images of electron density. The signals will be made using the Transit Satellite System. These satellites are in polar orbits at an altitude of approximately 1000 km. The map in Figure 6 has been produced to illustrate the location of potential ground locations with a typical northward and southward Transit satellite pass plotted over them.

Patricia Doherty will install and operate the receiver located in Bermuda during this campaign. In preparation for the campaign, a suitable Bermudan site was researched and selected. Training in the installation, maintenance, and operation of the equipment was also completed. In addition, modifications of a satellite prediction program were made for a more specific requirement.

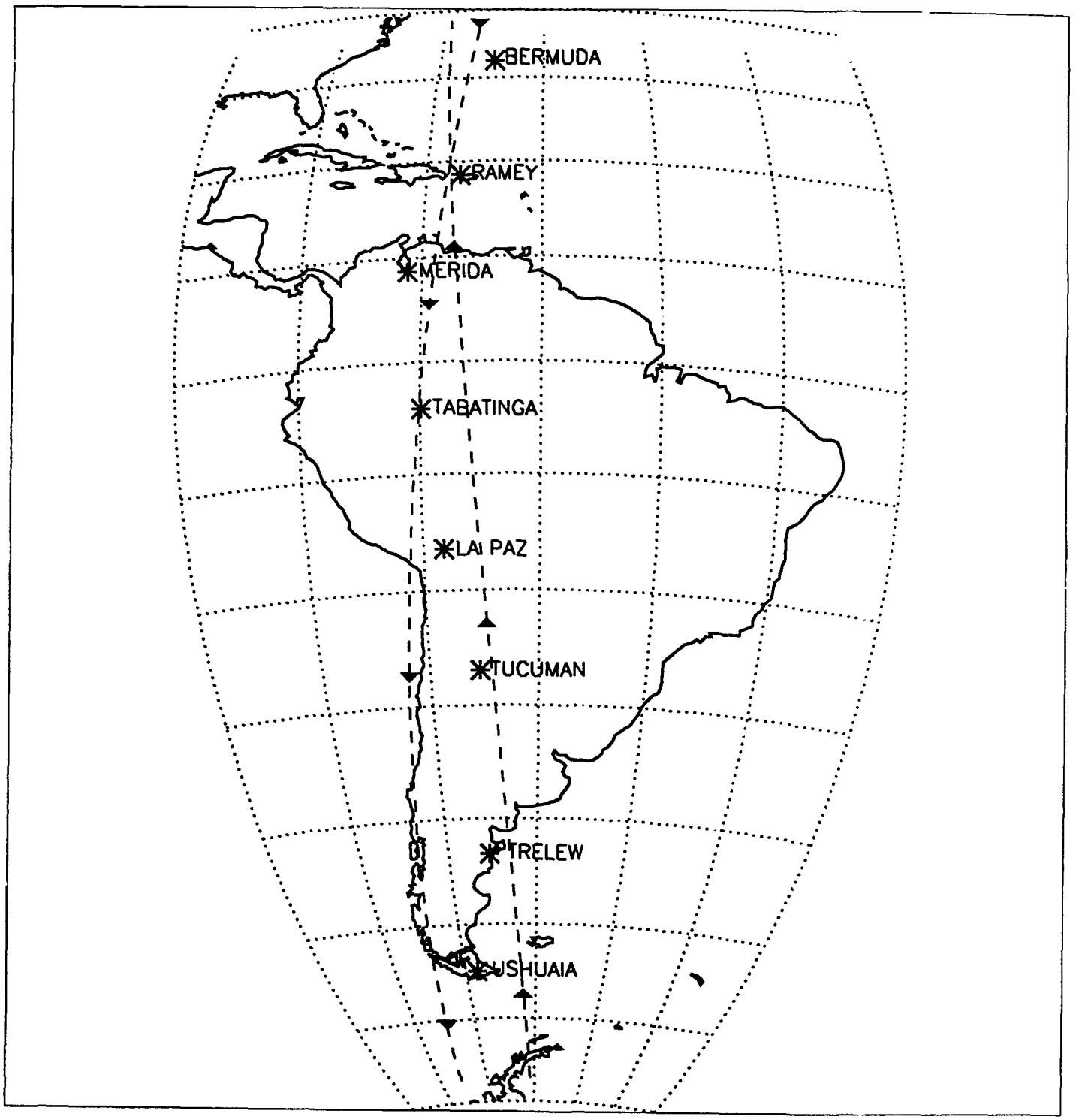
BERMUDA
RAMEY
MERIDA
TABATINGA
LA PAZ
TUCUMAN
TRELEW
USHUAIA

Figure 6

3. GPS OBSERVATIONS

3.1 Limitations in Making Absolute Ionospheric Measurements Using GPS

There are some serious potential problems in making accurate Total Electron Content (TEC) measurements using the L-band transmissions from the Global Positioning System (GPS) satellites. These limitations must be understood before ionospheric researchers can use the GPS dual frequency signals to obtain correct measurements of absolute total electron content.

The greatest problem in determining absolute TEC using GPS is in the calibration of the satellite differential group delay offsets. This value is called T_{gd}, and can be over 10^{17} el/m^2, or 10 TEC units. These space vehicle biases have been studied extensively by many ionospheric workers. None of the studies correlates with each other or with the pre-launch values. In addition, we have found that these biases change over a period of time. A possible method of using GPS signals for absolute TEC values is to continuously make independent measurements of T_{gd} and its variability. In an attempt to make progress on this problem, we have obtained data from other sites. In particular, we are interested in higher latitude data where we would expect that the plasmasphere would no longer play a role. The hope is that in this simpler situation, we can begin to make progress on the T_{gd} problem.

3.2 Ionospheric Corrections to Precise Time Transfer Using GPS

The ionosphere can be the largest source of error in GPS positioning and navigation. Radio waves propagating through the ionosphere suffer an additional time delay as a result of their encounter with the free electrons in the ionosphere. TEC is a function of many variables, including geographic location, local time, solar ultraviolet radiation, season, and magnetic activity. Accurate information on the behavior of TEC is important to satellite navigation and time transfer systems that correct for the time delay effects of the earth's ionosphere.

The GPS dual frequency system provides the opportunity to measure absolute TEC with a high degree of accuracy. Absolute TEC values are obtained by measuring the differential group delay of the 10.23 MHz modulation on the dual frequency signals. Relative TEC values are obtained by monitoring the differential phase of the two GPS carriers. By combining both the relative accuracy of the differential carrier phase with the absolute TEC obtained from the differential group delay, excellent absolute TEC measurements can be made. An example of this technique is illustrated in Figure 7. The group delay measurement for one complete satellite pass is plotted in Figure 7a. Note that this is an absolute measurement of time delay. However, it includes the effects of multipath and receiver noise. Figure 7b represents the relative, but highly accurate, phase measurement for the same satellite pass. Figure 7c illustrates the results of fitting the relative phase measurement to the absolute, but noisy, group delay measurement to obtain a highly accurate measure of absolute ionospheric time delay.

We have recently completed a study on the variability of TEC using this technique. The data were recorded at Hanscom AFB MA using the four channel ICS-4Z Mini Rogue GPS dual frequency receiver. This receiver has a high performance design that is capable of tracking four satellites simultaneously using the P-codes on both frequencies, Ll and L2, in addition to the C/A code on the Ll frequency.

The GPS data used in this study were recorded from May 1992 through April 1993. Figure 8 illustrates the satellite paths of the various GPS satellites over Hanscom for

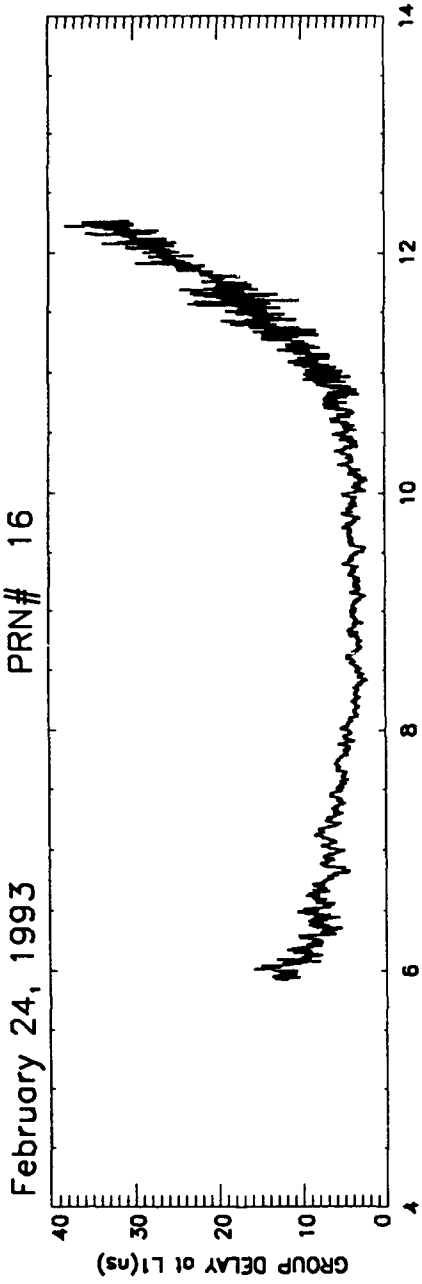

Figure 7a

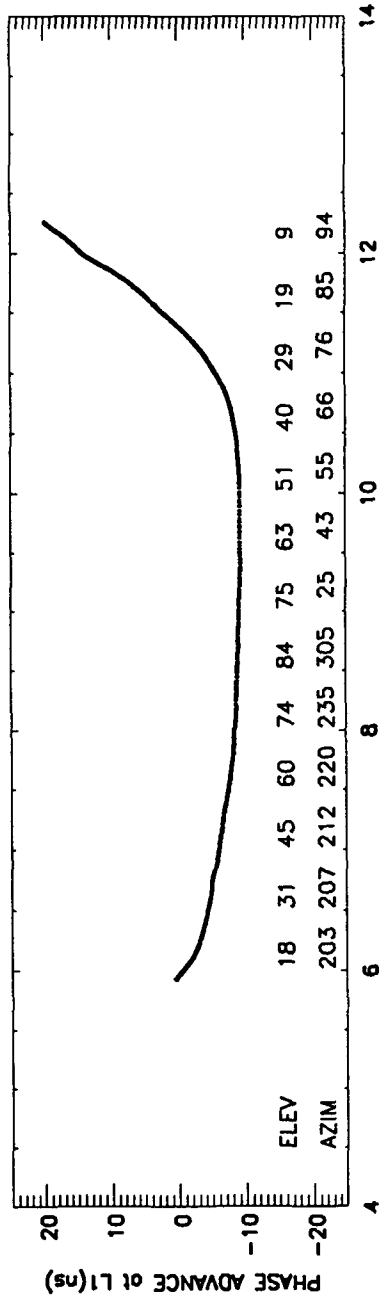

Figure 7b

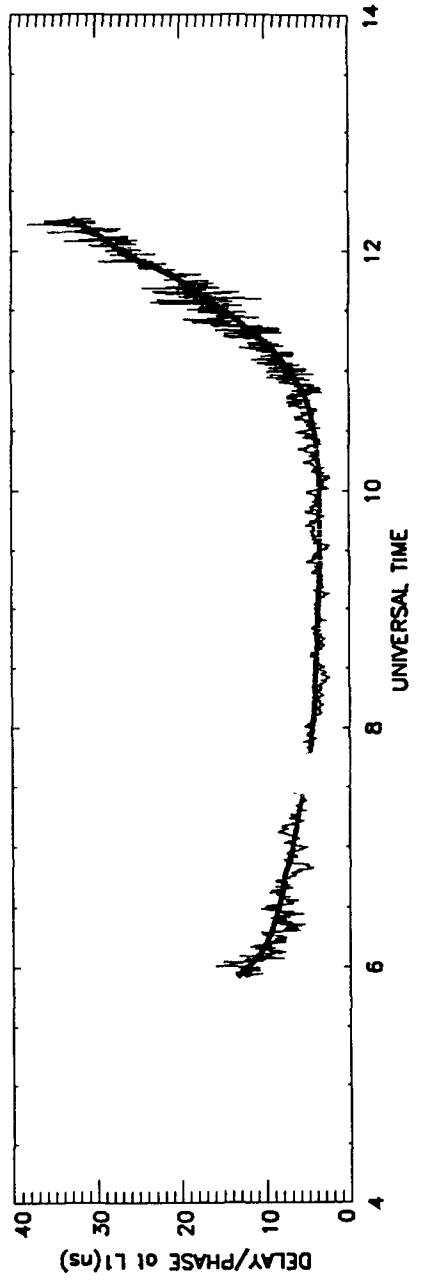

Figure 7c

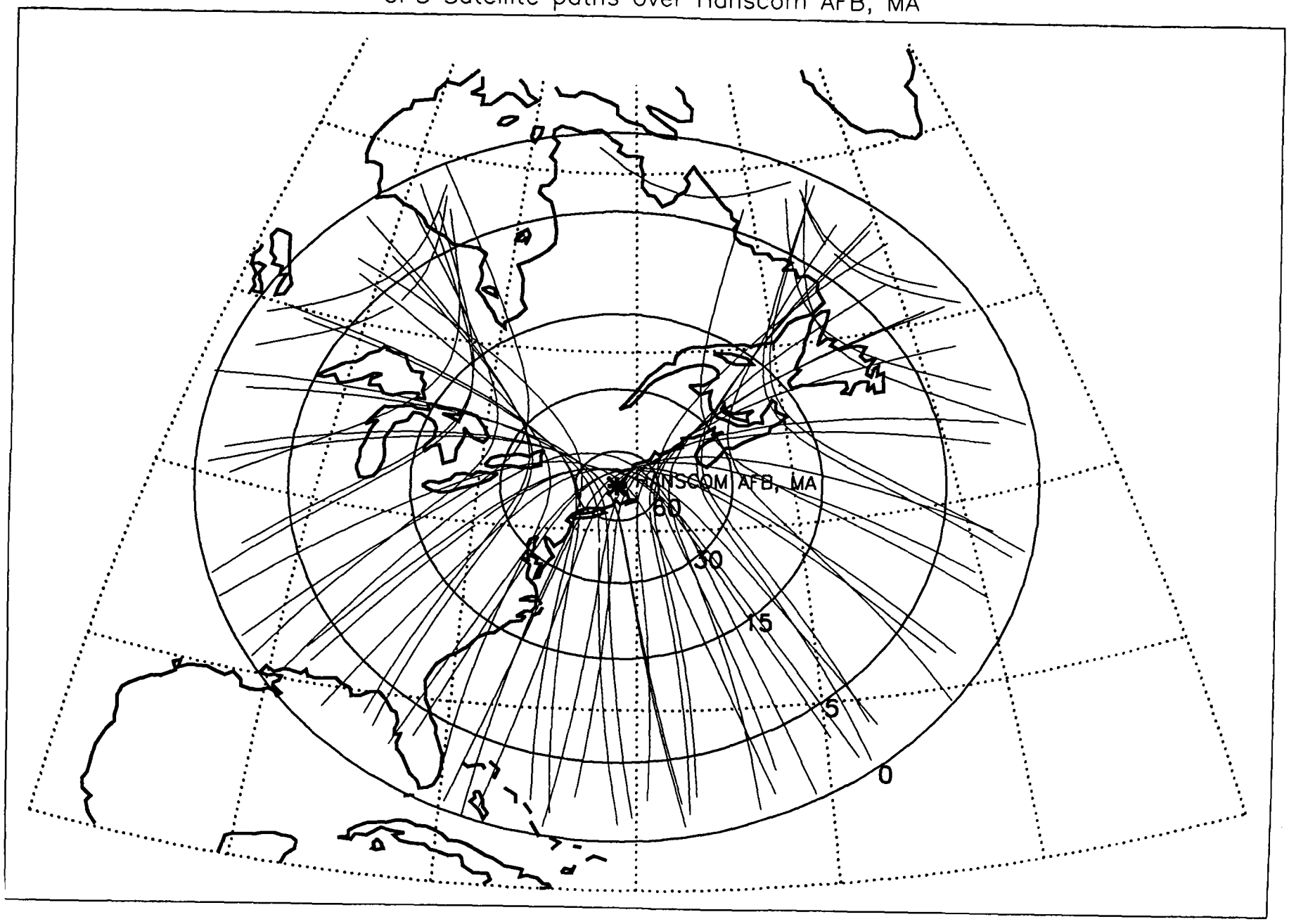
GPS Satellite paths over Hanscom AFB, MA
HANSCOM AFB, MA
60
30
15
5
0

Figure 8

one day during this period. Elevation angles of 0 through 60 degrees are represented by the concentric rings centered around the station. Satellite signals received from widely spaced azimuth and elevation angles pass through greatly different regions of the ionosphere. Therefore, simultaneous measurements of ionospheric time delay (or TEC) along different lines of sight generally are not the same.

Figure 9 displays the observations recorded on February 24, 1993. The slant absolute delay measurements have been converted to equivalent vertical time delay in ns at Ll. That is the measurement at the geographic position directly below the point where the satellite intersects the centroid of the electron density distribution with height, typically at 400 km. In order to display the diurnal variation of ionospheric time delay, the data are plotted versus the local time at this sub-ionospheric intersection point. At any local site, the ionization generally peaks in the mid-afternoon hours, and drops rapidly at night. The differences between measurements made at the same local time are attributed to the ionospheric gradients encountered by satellite paths intersecting the ionosphere at different latitudes.

Ionospheric time delay is highly variable by season. Figure 10 illustrates the statistics of ionospheric time delay for three seasons during the daytime hours of 1100-1700 local time. The daytime TEC values were computed and grouped by season: summer (May through August), winter (November through February), and the combined equinoxes of March, April, September and October. The ionospheric time delay measurements are plotted against their cumulative probability so that the percentage of occurrence above and below certain probability levels can be observed. A straight line on this type of statistical plot indicates a normal distribution. The slope of the line is a measure of the standard deviation, and departures from a straight line are simply deviations from a normal distribution. This figure indicates that the median daytime values of ionospheric time delay are highest in winter, followed closely by the equinox period. The summer values are the lowest. The winter season exhibits a significant departure from a normal curve above the 99% probability point. Departures like these are often due to the effects of magnetic storm activity.

Figure 11 illustrates the statistics of ionospheric time delay during the nighttime hours of 2300-0500 local time. Here, it is evident that the summer nighttime values are higher than those of the other two seasons. Winter and equinox have a more nearly normal distribution than summer. Summer begins to depart significantly from a normal distribution above the 95% probability level. The negative numbers below the 1% probability point are likely due to incorrect satellite biases.

Ionosphere time delay is primarily a function of solar ultraviolet radiation. A reasonable surrogate measure of the amount of ultra-violet radiation produced by the sun which is responsible for ionizing the earth's atmosphere, and producing the ionosphere, is the number of sunspots visible on the solar surface. Figure 12 illustrates the last two solar cycles with the period indicated during which the GPS measurements were made. This period was in the declining phase of the current solar cycle. Therefore, the ionospheric time delay values measured are approximately half the magnitude expected at the peak of the solar cycle.

The data set used in this ionospheric variability study is the first continuous, well-calibrated, dual frequency GPS ionospheric data set large enough for statistical research. The TEC parameter, however, has been studied for over twenty years using measurements of the Faraday rotation of linearly polarized radio waves transmitted from geostationary satellites. For comparison with the GPS TEC study, Figure 13 is included to represent the daytime probability of equivalent vertical ionospheric time delays at the GPS Ll frequency,

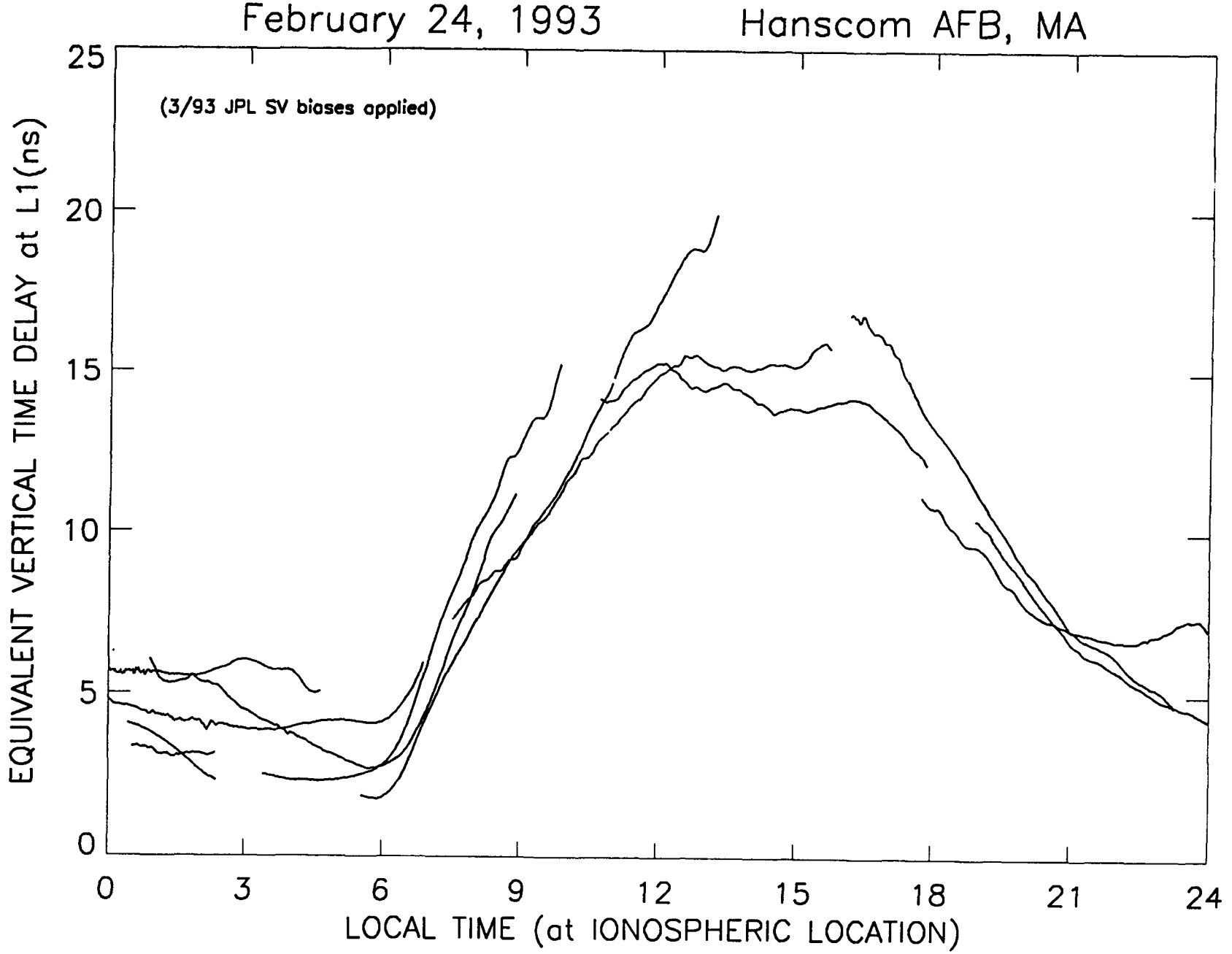
February 24, 1993
Hanscom AFB, MA
(3/93 JPL SV biases applied)
EQUIVALENT VERTICAL TIME DELAY at L1(ns)
25
20
15
10
5
0
0
3
6
9
12
15
18
21
24
LOCAL TIME (at IONOSPHERIC LOCATION)

Figure 9

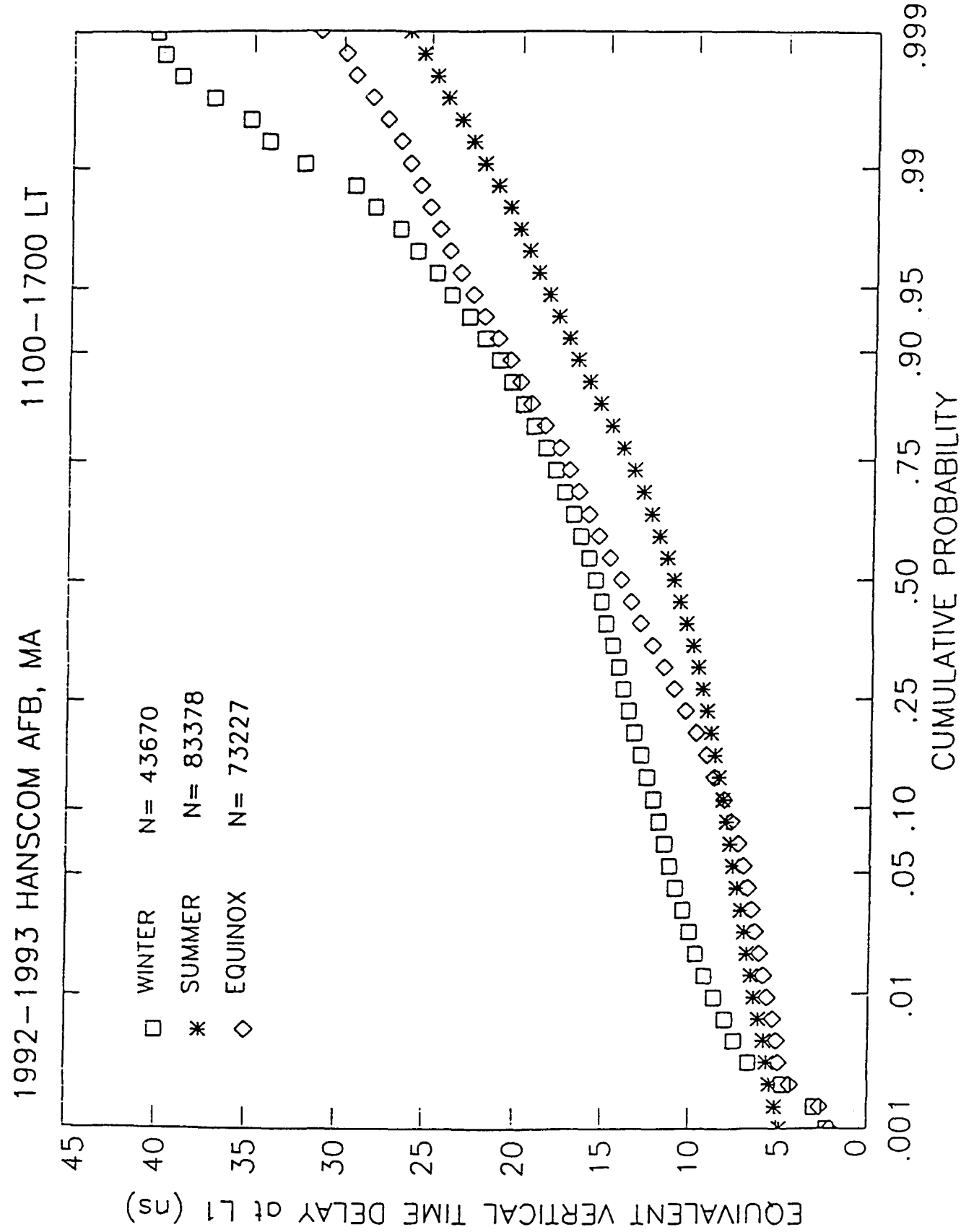
1992–1993 HANSCOM AFB, MA
1100–1700 LT
WINTER N= 43670
SUMMER N= 83378
EQUINOX N= 73227
EQUIVALENT VERTICAL TIME DELAY at L1 (ns)
CUMULATIVE PROBABILITY
45
40
35
30
25
20
15
10
5
0
.001
.01
.05
.10
.25
.50
.75
.90
.95
.99
.999

Figure 10

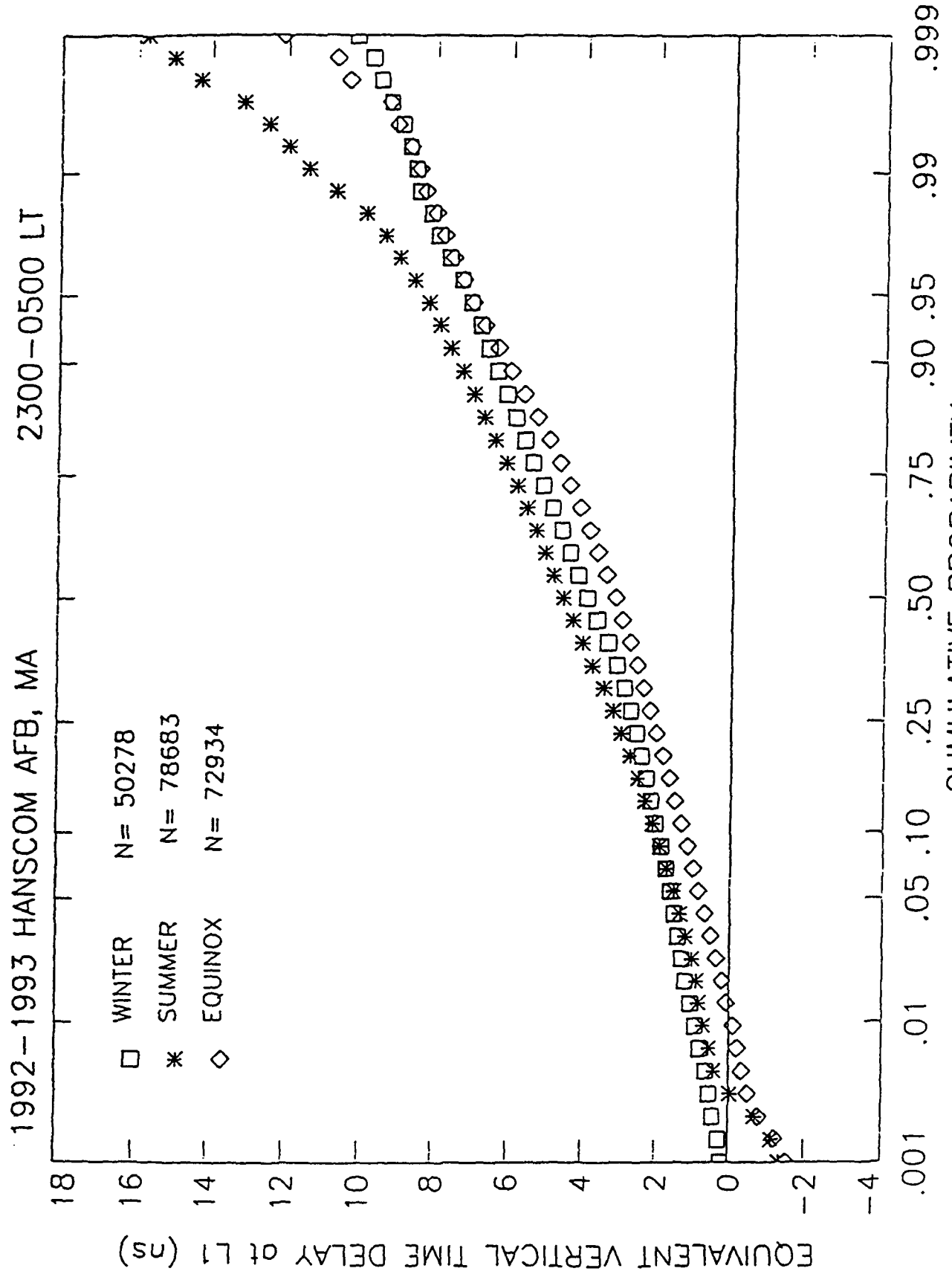
1992–1993 HANSCOM AFB, MA
2300–0500 LT
WINTER N= 50278
SUMMER N= 78683
EQUINOX N= 72934
EQUIVALENT VERTICAL TIME DELAY at L1 (ns)
CUMULATIVE PROBABILITY
18
16
14
12
10
8
6
4
2
0
−2
−4
.001
.01
.05
.10
.25
.50
.75
.90
.95
.99
.999

Figure 11

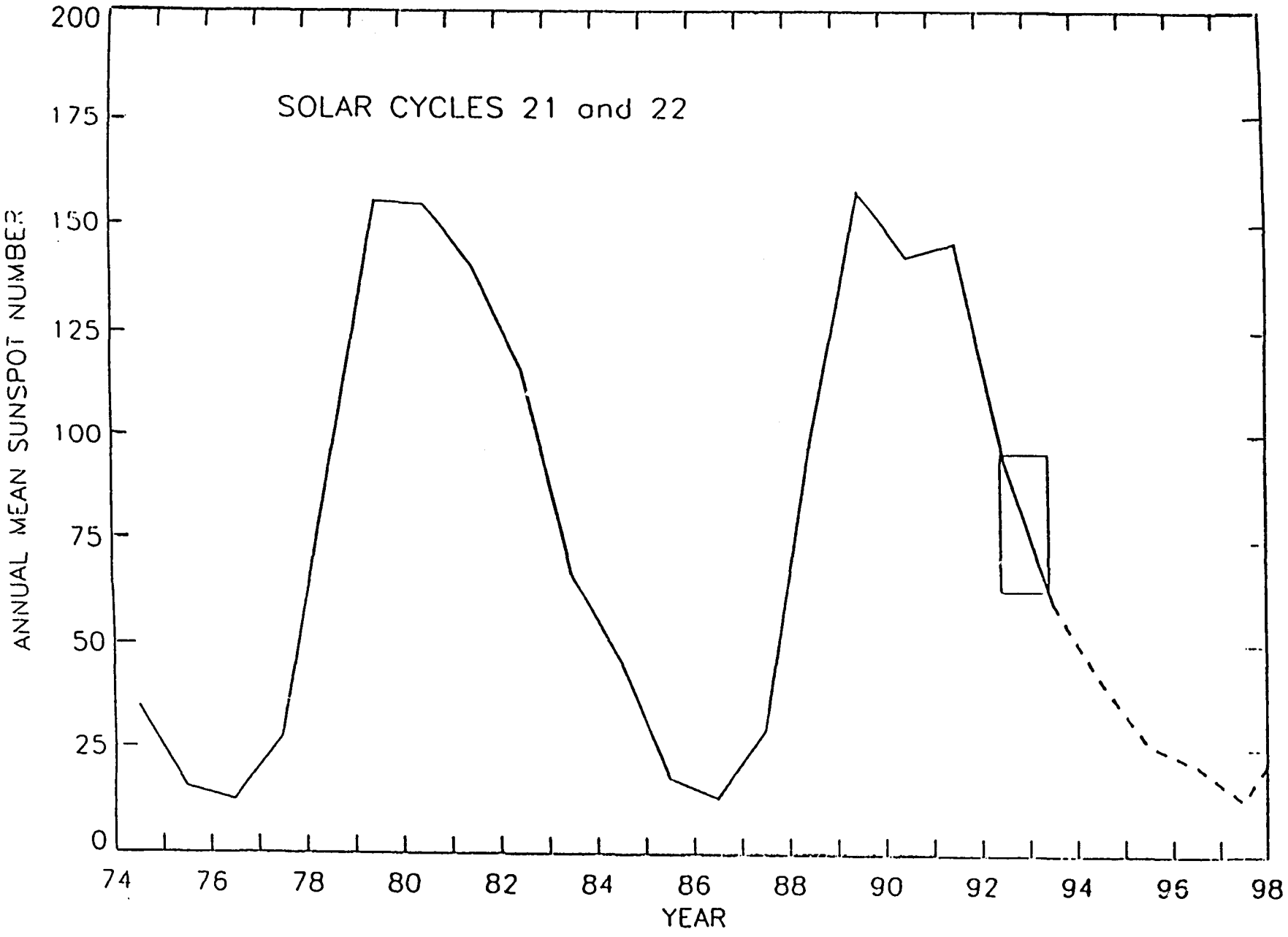
SOLAR CYCLES 21 and 22
ANNUAL MEAN SUNSPOT NUMBER
200
175
150
125
100
75
50
25
0
74
76
78
80
82
84
86
88
90
92
94
96
98
YEAR

Figure 12

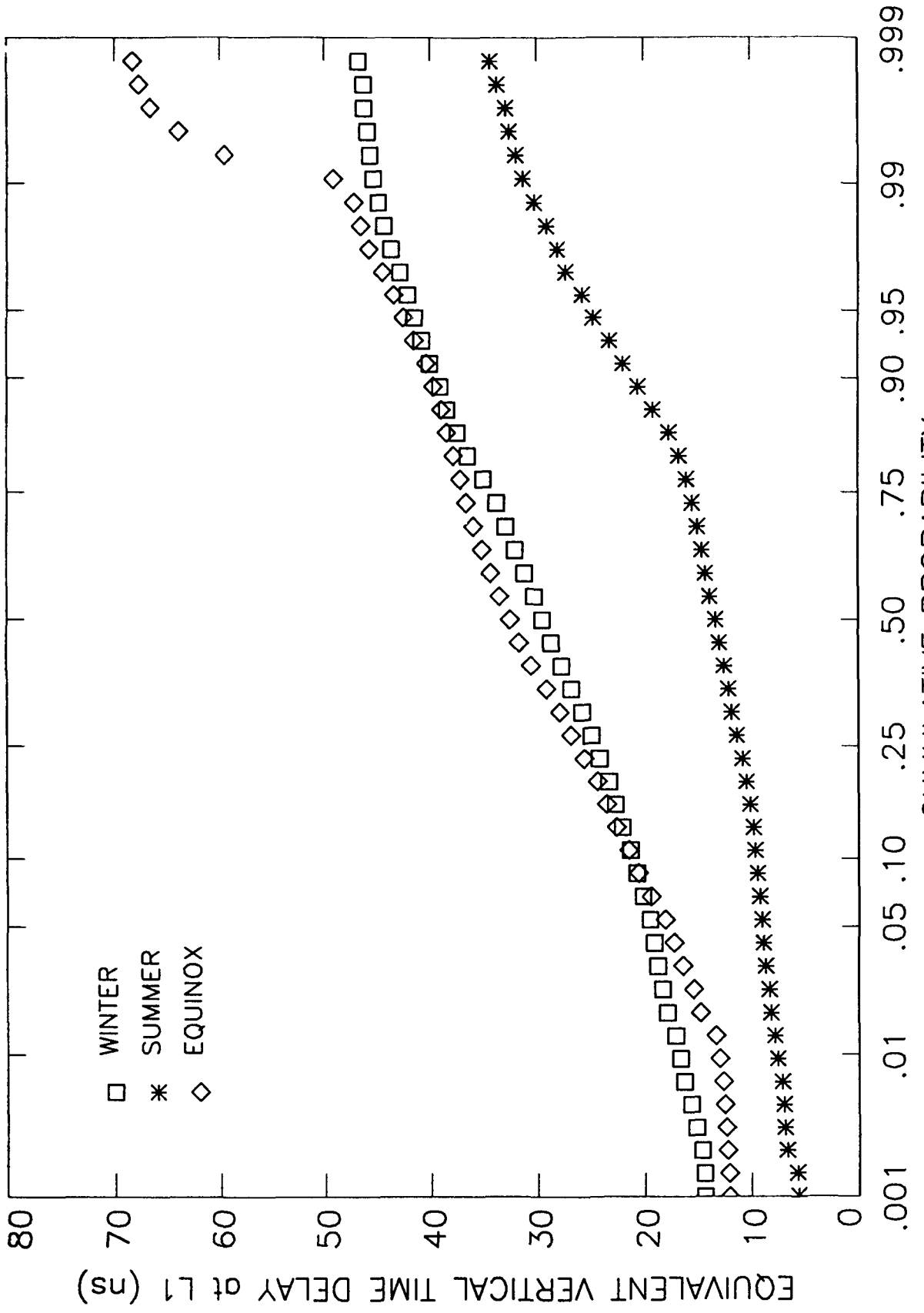
1981 Hamilton, MA 1100–1700 LT
WINTER
SUMMER
EQUINOX
EQUIVALENT VERTICAL TIME DELAY at L1 (ns)
80
70
60
50
40
30
20
10
0
.001 .01 .05 .10 .25 .50 .75 .90 .95 .99 .999
CUMULATIVE PROBABILITY

Figure 13

as determined from the Hamilton MA 1981 Faraday rotation data. A comparison of these 1981 results and the recent GPS daytime statistics (Figure 10) illustrates agreement in seasonal behavior with summer producing the smallest daytime values and equinox exhibiting the greatest day-to-day variability. It also illustrates the ionospheric time delay dependence on solar activity, with the 1981 data producing median values that are nearly two times those encountered during the 1992-1993 period.

3.3 GPS Data Analysis

The Jet Propulsion Laboratory operates a bulletin board containing dual-frequency GPS measurements for the globally located receivers in the GPS International Tracking Network.

All data recorded by the network are written in Receiver Independent Exchange Format (RINEX). Near the end of this year, programs were written to:

1) convert the RINEX format to phase and pseudorange in TEC units,

2) calculate azimuth and elevation for all data samples,

3) determine absolute TEC by fitting the smooth/relative phase data to the noisy/absolute pseudorange data using an arithmetic mean fit,

4) test for and remove phase cycle slips,

5) plot the results.

Figure 14 illustrates the results of this analysis for four satellite passes recorded in the Northwest Territories on November 13, 1993. The highly fluctuating curve displayed in each pass is the noisy pseudorange data. The smooth curve is the absolute TEC measurement determined by the arithmetic fit of the phase to the pseudorange data. The station recording this sample of data is located at 62 degrees north and is likely experiencing auroral effects.

The data from this network provide numerous opportunities for ionospheric research. Plans are currently being developed to use a portion of this data to investigate the problem discussed in Section 3.1 concerning individual space vehicle offsets in the GPS Satellites.

3.4 Static Ionospheric Test for the WADGPS Experiment

We have supported the FAA's Phase 1 Wide Area Differential GPS (WADGPS) Satellite Navigation Testbed Experiment by operating a GPS receiver at Hanscom AFB, analyzing the measured data, and providing the results to the Mitre Corporation.

Support also consisted of delivering a revised version of the data analysis program to the FAA. The new version of the processing software improved data error detection and run time. This program is used by our site and three other sites operated by the FAA in their WADGPS experiment.

Our first study of this WADGPS data has consisted of analysis of a year's worth of data with the purpose of assessing some of the current limitations to Wide Area Differential GPS. These data were collected from May 1992 through April 1993 at the following locations:

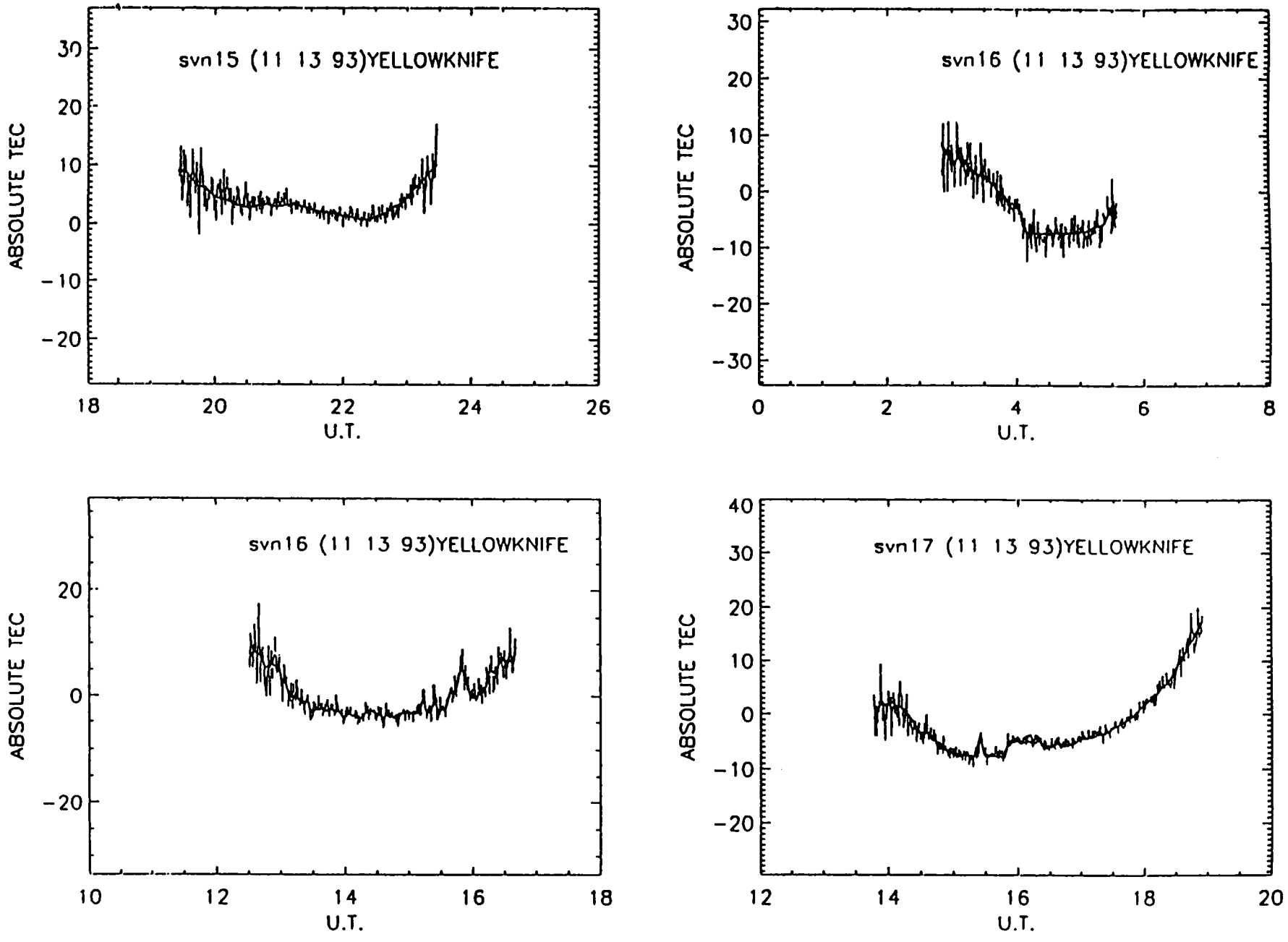
svn15 (11 13 93)YELLOWKNIFE
ABSOLUTE TEC
U.T.
svn16 (11 13 93)YELLOWKNIFE
ABSOLUTE TEC
U.T.
svn16 (11 13 93)YELLOWKNIFE
ABSOLUTE TEC
U.T.
svn17 (11 13 93)YELLOWKNIFE
ABSOLUTE TEC
U.T.

Figure 14

Oldtown, ME	(44.95 North, 68.67 West)
Hanscom AFB, MA	(42.45 North, 71.27 West)
Atlantic City, NJ	(39.45 North, 74.57 West)
Dayton Airport, OH	(39.90 North, 84.22 West)
Georgetown, SC	(33.31 North, 79.32 West)

One of the major issues in WADGPS is to determine the number and placement of ionospheric monitoring stations in the Continental United States (CONUS) required to represent the ionospheric range error between stations to within a specific value. One of the potential limitations in WADGPS is the unknown spatial variability of ionospheric range errors between locations where dual frequency GPS measurements are being made.

The important parameter in this study is the difference in range error as a function of distance. Thus, differences in the received absolute range error viewing the same GPS satellites from two different locations were computed. Pairs of points using common GPS satellites were used in order to keep the approximate same distance between the ionospheric intersection as the station spacing, since the viewing angles to the satellites are nearly parallel for stations spaced within the region of our experimental work.

Figure 15 illustrates some of the results of this study. It shows the statistical behavior of the differences in range error, in meters, for the Hanscom AFB, Atlantic City Airport station pair. Differences in range error are plotted separately for each of three seasons: summer (May through August), winter (November through February), and the combined equinoxes (March, April, September and October). The data were further separated into daytime, 11-17 hours local time, and nighttime, 23-05 hours local time. These differences are plotted against their cumulative probability so that the percentage occurrence below and above certain probability values can easily be seen. Figure 15 shows that the ionospheric range error differences at the 1% cumulative probability point are approximately -2 meters, the median difference is -1 meter, and the difference at the 99.9% cumulative probability point is about 1 meter. Therefore, the absolute difference in range error for this data set was virtually always less than 2 meters. The distance between Hanscom AFB and Atlantic City Airport is approximately 434 kms.

Figure 16 illustrates the results using the Dayton, Ohio and Hanscom AFB station pair. It shows that the absolute difference in range error measured at these two stations is higher than 2 meters at the 25% cumulative probability point for two seasons and exceeds 6 meters at the 1% point. The median point, however, is still less than 2 meters. The higher numbers are a result of the greater distance between this station pair. The distance between Dayton and Hanscom AFB is 1,120 km.

Similar figures are currently in process for all the station pairs listed above.

Unfortunately, the current portion of the present solar cycle during which our measurements were taken was not a period of maximum solar activity, but was approximately halfway down the descending phase of the current cycle of high activity. For a period of very high solar activity, the range errors, and the corresponding differences in range errors between pairs of stations, will be a factor of 2 higher than those actually observed and reported in this report.

The largest values of absolute ionospheric range error, and the largest temporal and spatial gradients, generally occur during magnetic storms, especially during major magnetic storms. During the period of measurement here, from May 1992 through April 1993, there were a number of magnetic storms. None, however, was considered to be major magnetic

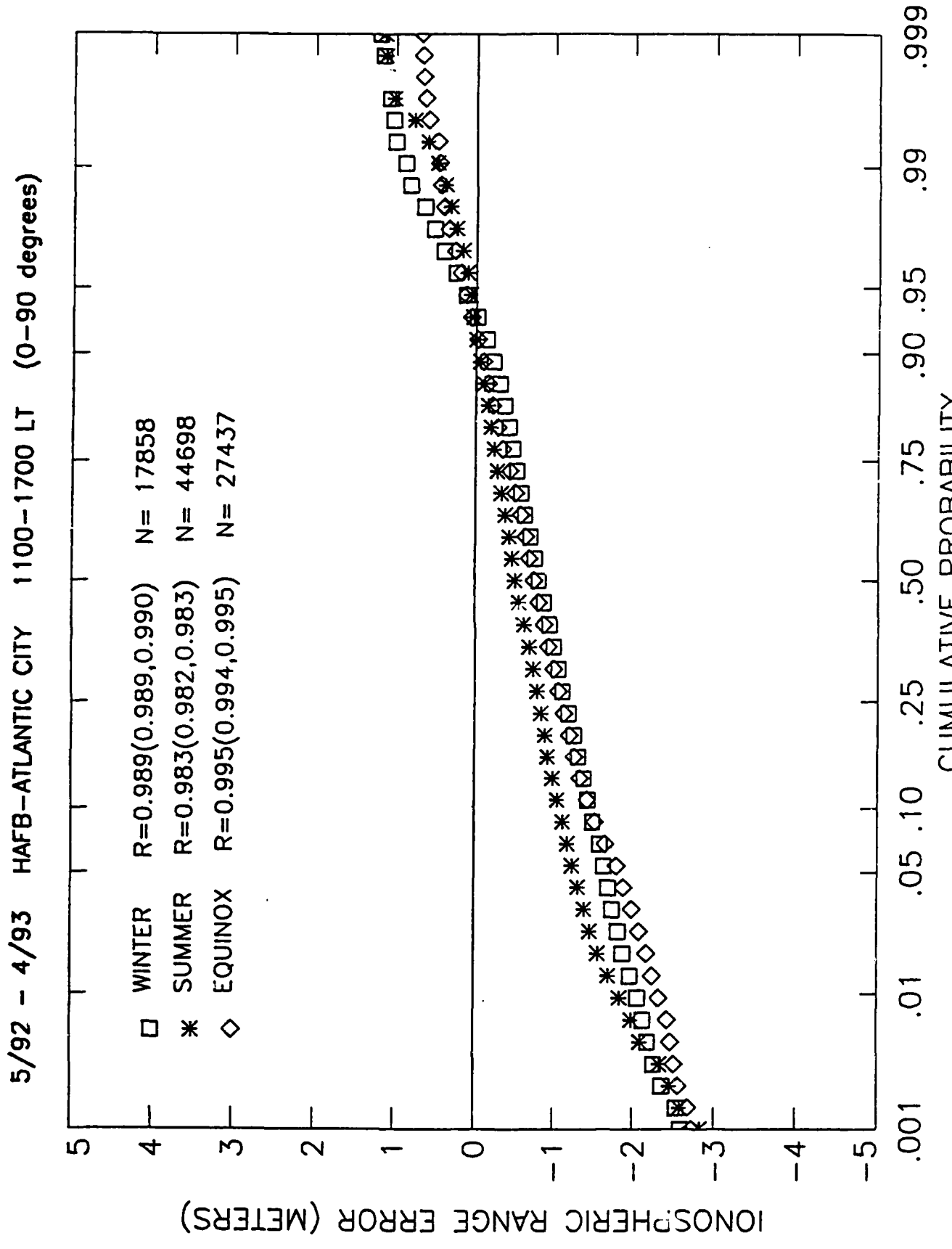
5/92 - 4/93 HAFB-ATLANTIC CITY 1100-1700 LT (0-90 degrees)
WINTER R=0.989(0.989,0.990) N= 17858
SUMMER R=0.983(0.982,0.983) N= 44698
EQUINOX R=0.995(0.994,0.995) N= 27437
IONOSPHERIC RANGE ERROR (METERS)
CUMULATIVE PROBABILITY
5
4
3
2
1
0
-1
-2
-3
-4
-5
.001
.01
.05
.10
.25
.50
.75
.90
.95
.99
.999

Figure 15

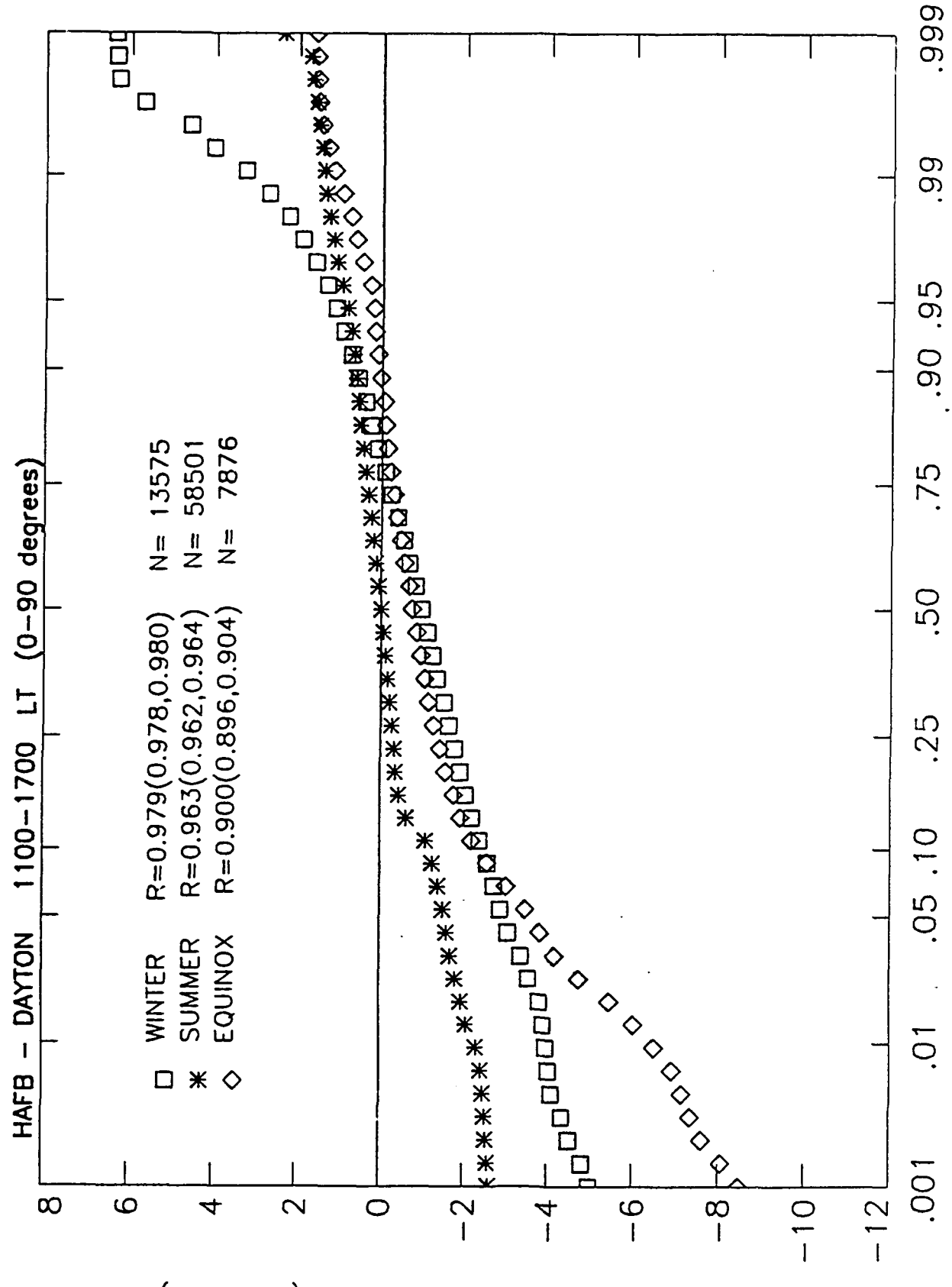
HAFB – DAYTON 1100–1700 LT (0–90 degrees)
WINTER R=0.979(0.978,0.980) N= 13575
SUMMER R=0.963(0.962,0.964) N= 58501
EQUINOX R=0.900(0.896,0.904) N= 7876
IONOSPHERIC RANGE ERROR (METERS)
CUMULATIVE PROBABILITY
8
6
4
2
0
-2
-4
-6
-8
-10
-12
.001
.01
.05
.10
.25
.50
.75
.90
.95
.99
.999

Figure 16

storms. During storms, the largest absolute differences in range error generally only occur during the late afternoon hours of the first day of the storm. If only a few major storms occur each year, and if the largest gradients occur only for a few hours during the storm, that cumulative length of time is less than one percent of the entire year. Thus, the ionospheric range error statistics will not be seriously affected except below the 1% and above the 99% levels. Little evidence of major storm effects was found at any probability point during our one-year of GPS range error measurements. This is a hopeful sign. Figure 17a illustrates the cumulative probability of TEC for local daytime hours for the entire month of April at Atlantic City. Figure 17b is the same data with the exception of the two storm days. A comparison of these two figures reveals deviations from normal behavior beginning at about the 90th percentile, with a maximum of approximately 9 meters at the 99th percentile.

An example of disturbances caused by storm activity is illustrated in Figure 18. Figure 18a illustrates range error measurements recorded at Hamilton MA during solar maximum using the Faraday technique. The large departure from a "normal" distribution above the 99% probability point is the result of a severe storm that occurred on October 18, 1981. Figure 18b illustrates the same data with the October 18th storm period removed, thus restoring the normal distribution.

Our initial results from the first year of measurements of ionospheric range error in the eastern CONUS region have shown that differential range errors are less than 2 meters for station spacings of approximately 430 kms for at least 99% of the time. Thus, stations to be used in an operational WADGPS should be located no greater than 430 km apart.

Work is continuing in this experiment. Additional data are being recorded at all 5 stations. We are also still working on data reduction for some of the data already collected. This type of study is useful because information on the ionospheric response to magnetic activity will aid the FAA in determining operating procedures during these disturbances.

4. ELECTRON BACKSCATTER AND PROTON PRECIPITATION

These two topics are combined because early in the year we wrote a manuscript entitled, "Upgoing Electrons Produced in an Electron-Proton-Hydrogen Atom Aurora". The purpose of this paper is to present the first test of a fully coupled electron-proton-hydrogen atom transport model. Specifically, we modeled the upgoing electrons that result from downgoing electrons and protons incident at the top of the ionosphere for a "nearly pure" proton aurora. Measurements from the Low Altitude Plasma Instrument (LAPI) onboard the Dynamics Explorer 2 satellite provide both the needed boundary conditions (incident electron and protons fluxes) and the resultant upgoing electron fluxes with which the model results are compared. We found that the agreement between data and theory can be characterized as good (10-40%). Given this agreement, we concluded that the data support the theoretical prediction that the secondary electron spectra, due to the precipitating protons and H atoms, is much softer than that produced by precipitating electrons.

However, before we submitted this paper, several issues arose concerning the proton-hydrogen atom transport (PHT) model that had to be addressed. They included an apparent inability to conserve energy to any better than 20%, and some unexpected behavior as a function of the energy grid used.

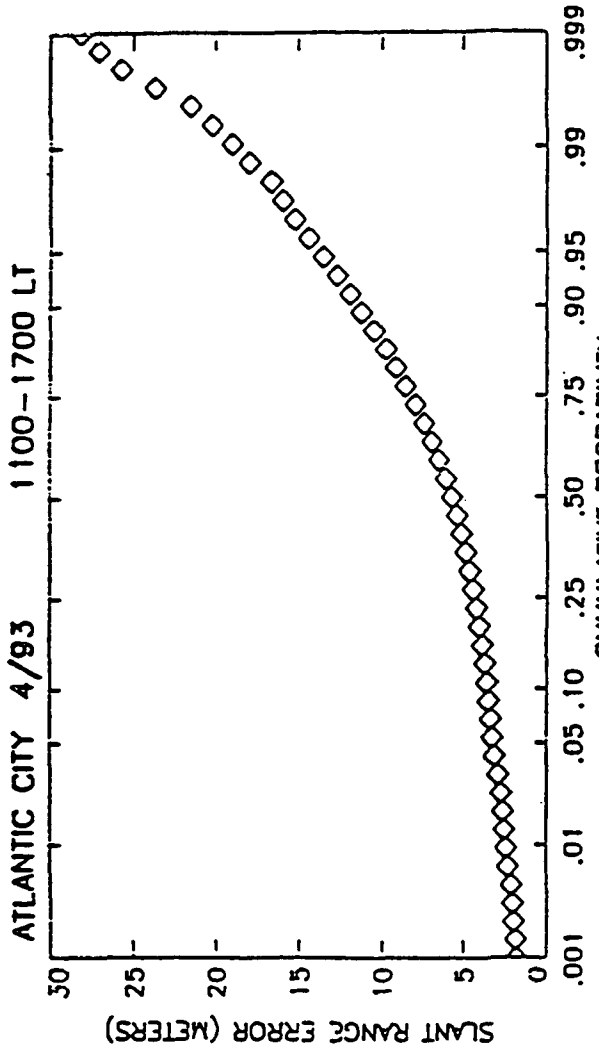

Figure 17a

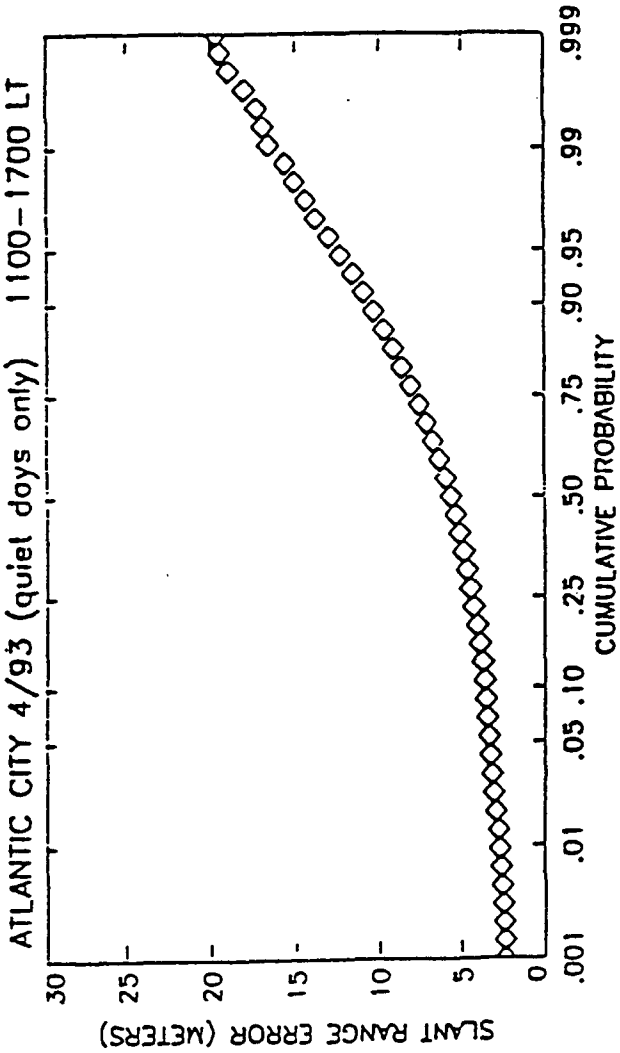

Figure 17b

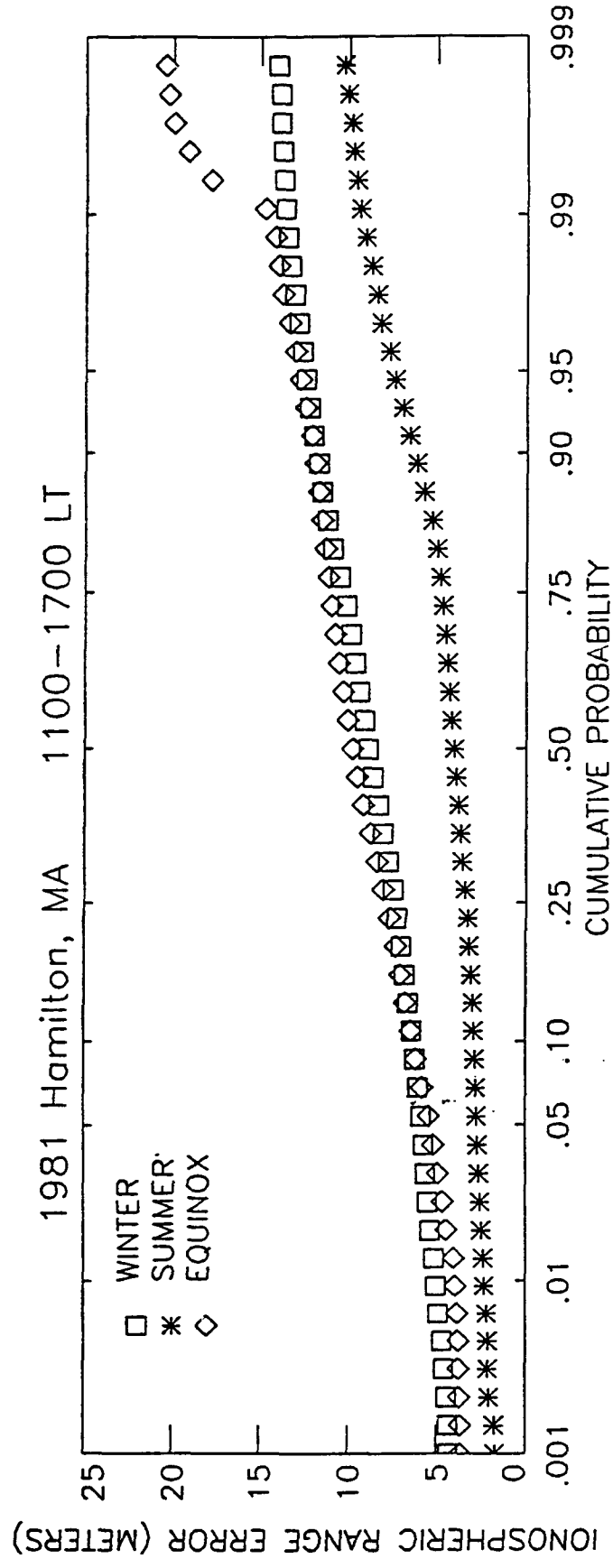

Figure 18a

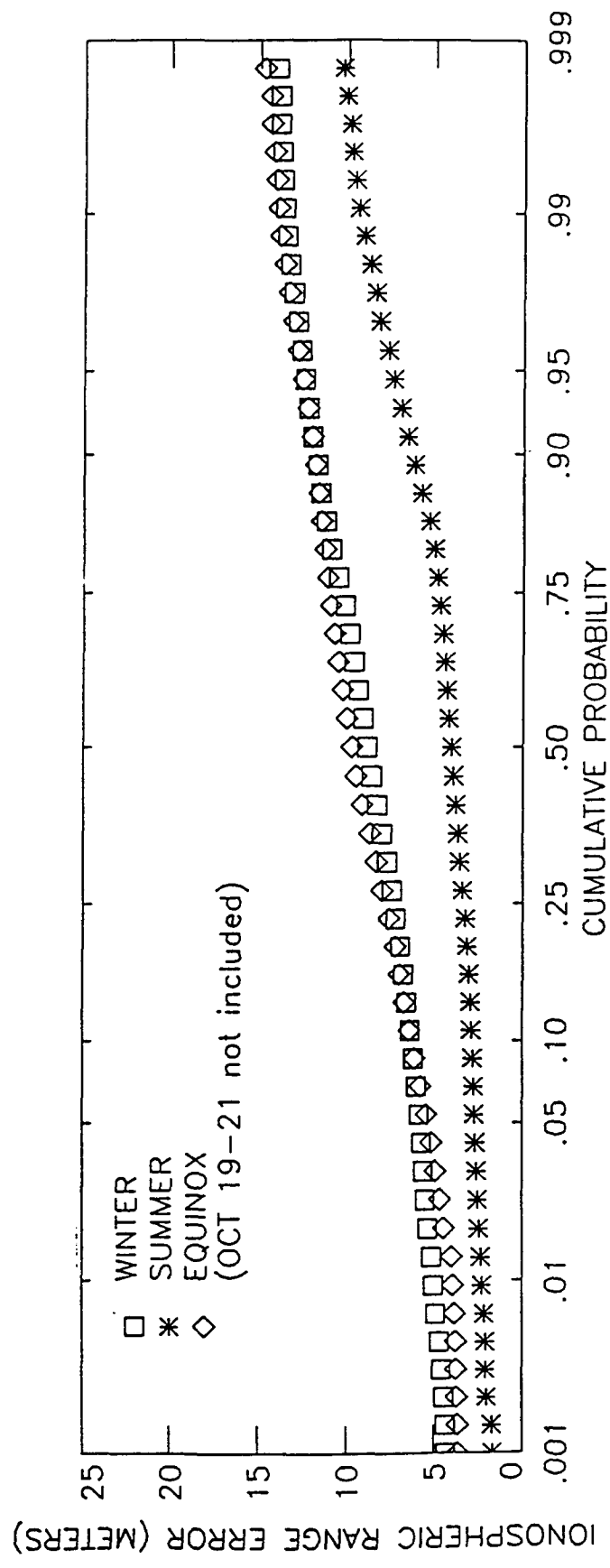

Figure 18b

4.1 Proton-H Atom Transport Model Developments

As mentioned, during the year several issues arose concerning the PHT model. The simplest problem was that of inconsistent behavior in the secondary electron spectrum produced in a proton aurora as a function of the energy grid used. This proved to be a minor bug in the handling of the relevant cross sections and was easily corrected. Of greater concern was the question of how well does the program conserve particles and energy.

To study this problem, we carefully formulated statements of particle and energy conservation that could be used in testing the solutions of the transport model. In using our implementations of the conservation laws to study this problem, a series of bugs were found in the code. Some proved to be minor but three were crucial. One involved the conservation tests themselves and the other two the basic integration over altitudes that is performed when solving for the proton and H atom fluxes. The present code now conserves particles and energy at each altitude and pitch angle to better than 6%. At many altitudes, it is better than 1%. The code is now more robust having been run from as high in altitude as 700 km and as low in energy as 100 eV. Previously, 500 eV was our lower energy limit, and our top altitude had to be 600 km or below. The present limit of 100 eV is simply a result of our present cross sections having a 100 eV lower limit. Likewise, the 700 km is a limit simply because we have yet to try a higher boundary altitude.

While the initial testing of the model was performed on the Convex, the model has been ported to the VAX so it can be conveniently used with our entire suite of transport codes that reside on the VAX cluster. Another version of the proton-H atom model exists on the Convex that gives essentially the same results, but has been modified to run more efficiently. It will be ported to the VAX sometime in the next year. We also plan to port the model to a Sun Sparc workstation sometime this summer.

4.2 Proton-H Atom Transport: A Comparison of Theoretical Techniques

Having resolved the several nagging problems with the PHT model, we have proceeded with the comparison between PHT and the Monte Carlo model of the group at the Polar Geophysical Institute in Apatity, Russia.

When DTD returned from Apatity, Russia, he brought back results from calculations made by the Polar Geophysical Institute Monte Carlo Proton-H Atom Model (MCPH). For this study, our initial runs of the PHT model were designed for comparison to these MCPH results. The MSIS-86 neutral atmosphere parameters, the boundary top altitude, the lowest energy, the input energy flux, and the functional form (a Maxwellian) of the incoming proton flux that we used are identical to what was used in the MCPH calculations. The Russians made a series of runs with the characteristic energy of the input flux varying from 1 to 20 keV. We have made two calculations with characteristic energies of 2 and 8 keV. In both cases, we obtained what appears to be very good agreement between PHT and MCPH results. For example, in Figure 19 we show for the 8 keV case the energy deposition rates from the two models. We see that they are generally within 10% of each other with the altitudes of the peak rates being only 1.5 km apart. In Figure 20, we show for the same case, the flux fraction as a function of altitude. Again we see fairly good agreement. Similar results are seen in the 2 keV case. We hope also to compare hemispherically averaged and energy averaged fluxes, but these comparisons will require further results from Russia.

We have sent these results to Apatity and await their next set of calculations. For our part, we will be running cases at other characteristic energies, going to lower energies

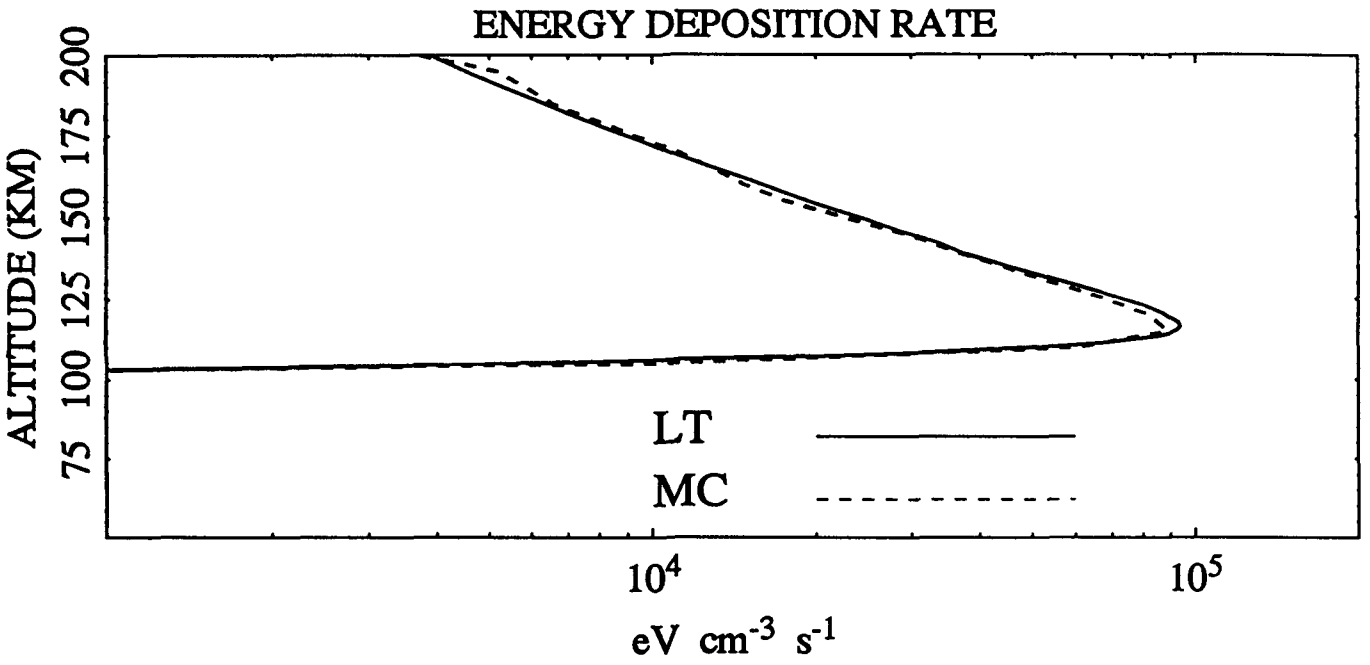

Figure 19

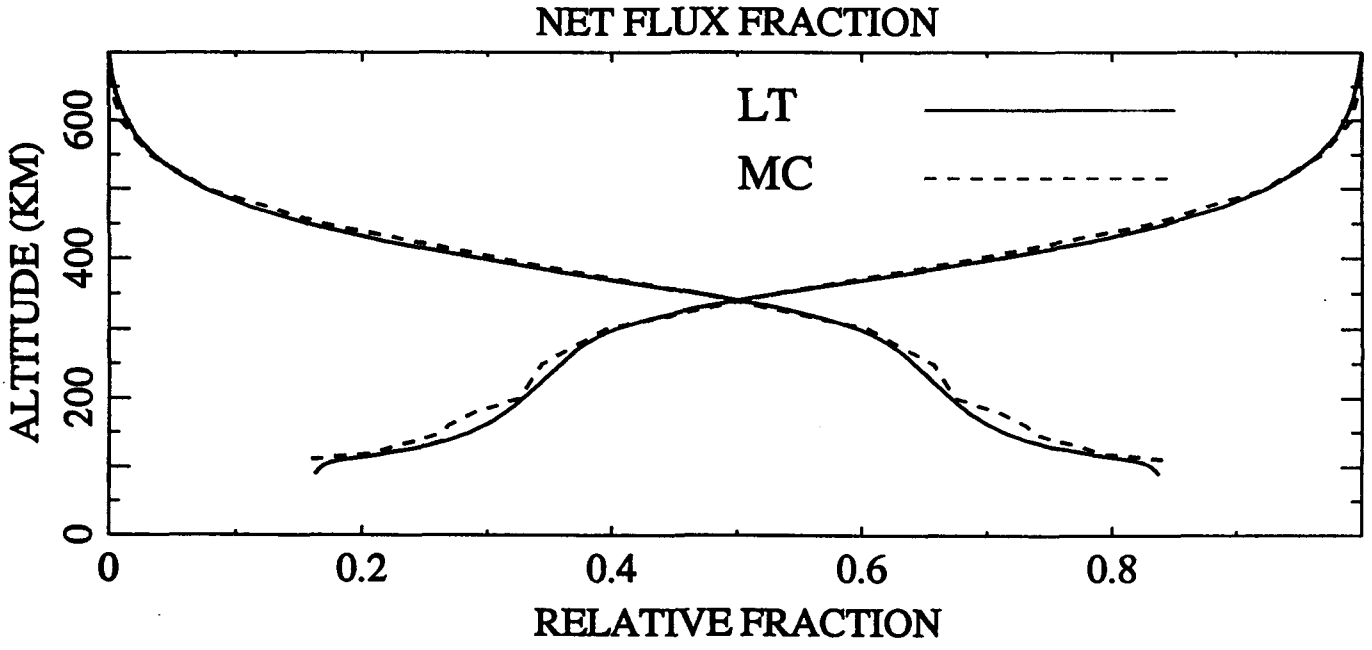

Figure 20

(100 eV), and testing sensitivity to cross sections. The Russians have expressed an interest in collaborating on a paper, and when this first set of calculations is completed, we should be in good shape for such an effort.

4.3 Electron-Proton-H Atom Aurora: Comparison With Observations

While a model for the electron-proton-hydrogen atom aurora now exists, comparisons between theory and experiment are in their infancy. Accordingly, we have been searching for suitable data to use in testing the combined electron-proton-H atom auroral model. Thus far, the results have been discouraging. Rocket shots made in the late sixties and early seventies have been disappointing in the quality of their data. The basic problem is the measurements do not provide a good specification of the inputs needed by the model nor many of the outputs needed for a through test of the model. Similarly, a recent rocket shot (ARIA) measured ion fluxes, but the counting statistics are so poor as to make modeling an altitude profile a pointless exercise.

One brief study using the proton-H atom transport model was completed. What was done was to use the Hardy et al. statistical model of auroral ion precipitation [1989] to supply the input proton fluxes to the model and then calculate the resulting Hβ emissions at various latitudes, local times, and magnetic activities. This was then compared to the empirical Hβ model of Creutsberg et al. [1988]. In Figure 21, we show a sample comparison where the dashed curves are from Creutsberg, and the solid curves are from the model calculations. The time given at the top is the local magnetic time and results are shown for three levels of magnetic activity. Going left to right, the solid curves are for Kp = 4, 2, 0 and the dashed curves are for ae = 360.1, 113.5, 25. One can see that the general trends with magnetic activity are consistent, but clearly the model results are running up to a factor of 2 higher. Given the uncertainties concerning ground-based measurements and the somewhat "apples and oranges" comparison that results from Hardy et al. being based on 18,000 satellite passes, and Creutsberg et al. being based on 14 nights, it is difficult to assess how serious a problem the model may have.

In another study, we attempted to model three emissions that were observed during the 1981 AFGL Auroral E rocket campaign. In this experiment, there were upward looking photometer measurements, but no successful particle measurements. This meant that we had to use one emission to determine the incident proton characteristics, another to determine the incident electron characteristics, and then using the inferred inputs calculate a third emission to compare to observation. In Figure 22, we show the fit to the Hβ emission assuming a 6.5 keV Maxwellian protons incident with an energy flux of .228 ergs/cm^2-sec. In Figure 23, we show the fit to 3914Å assuming 1.3 keV Maxwellian electrons incident with an energy flux of 1.6 ergs/cm^2-sec along with the incident protons. Finally in Figure 24, we show the VK 2762Å emission that results from using the inferred particle fluxes. The two curves come from using different O quenching factors. The S designates the aeronomically determined factor from Sharp, and the P designates the laboratory determined factor from Piper. One can see that within the quenching uncertainty, we have good agreement. It should be noted that while an encouraging result, this case is not a very severe test of the proton-H atom model since most of the emission appears to come from the electrons.

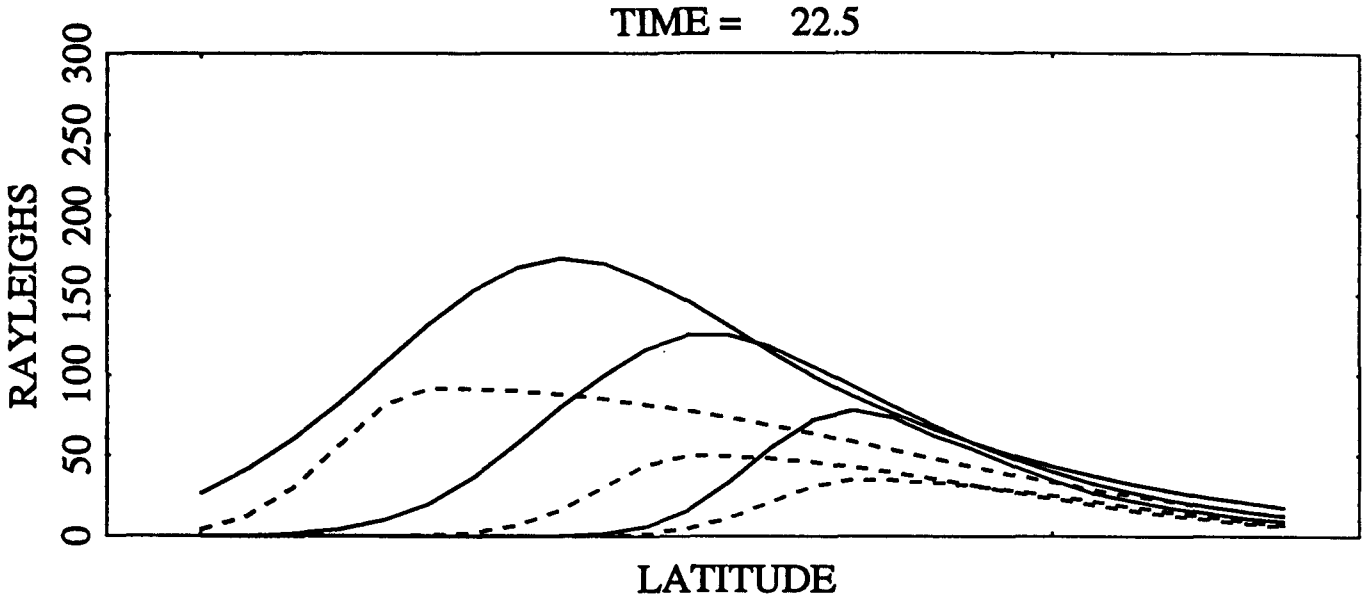

Figure 21

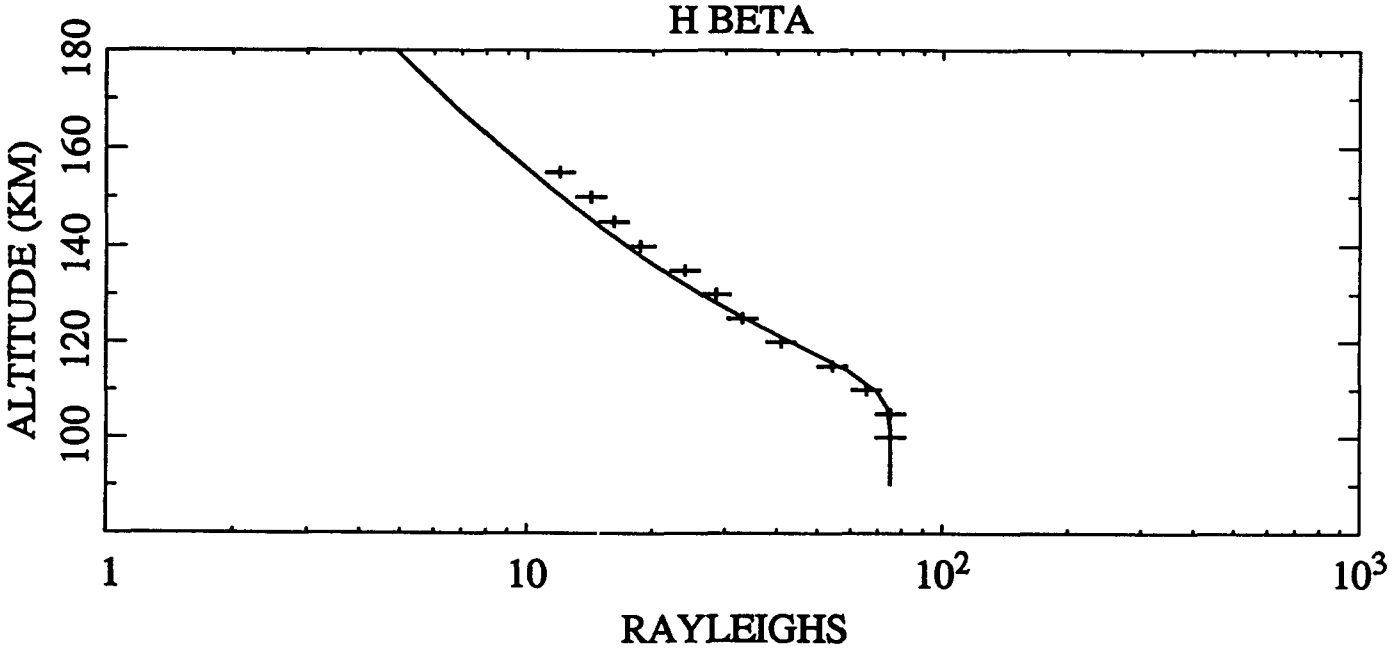

Figure 22

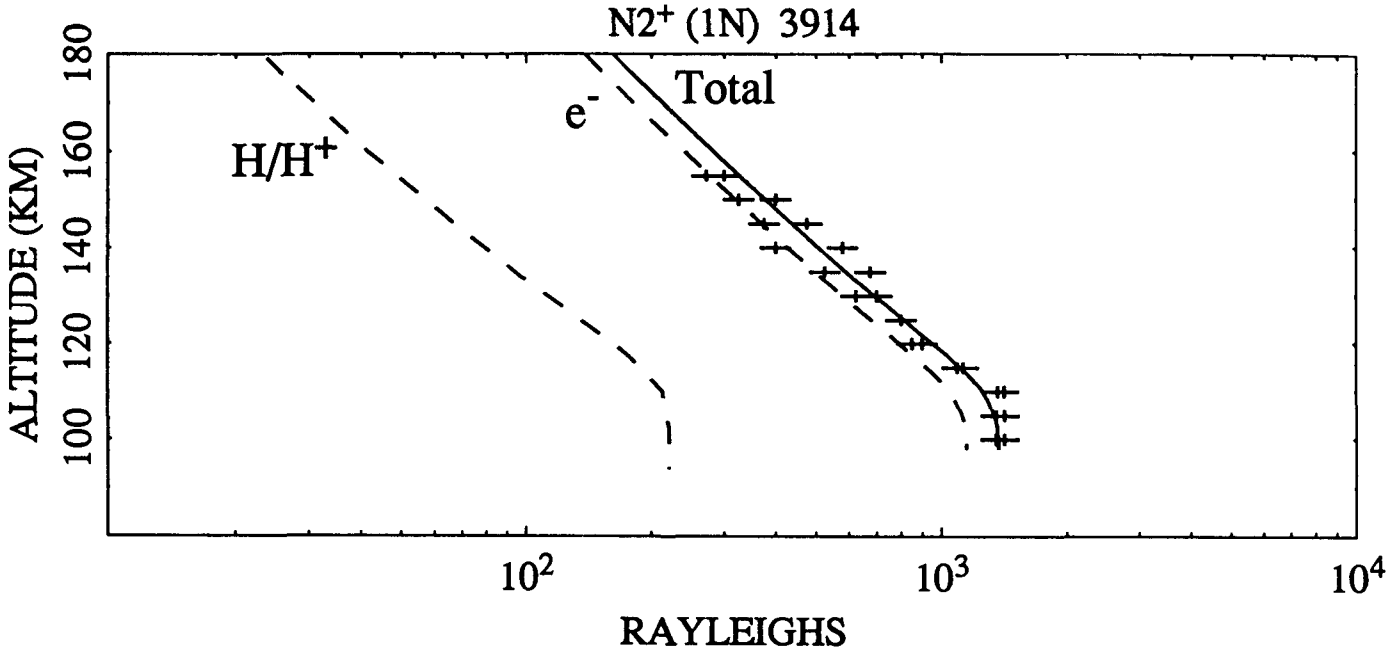

Figure 23

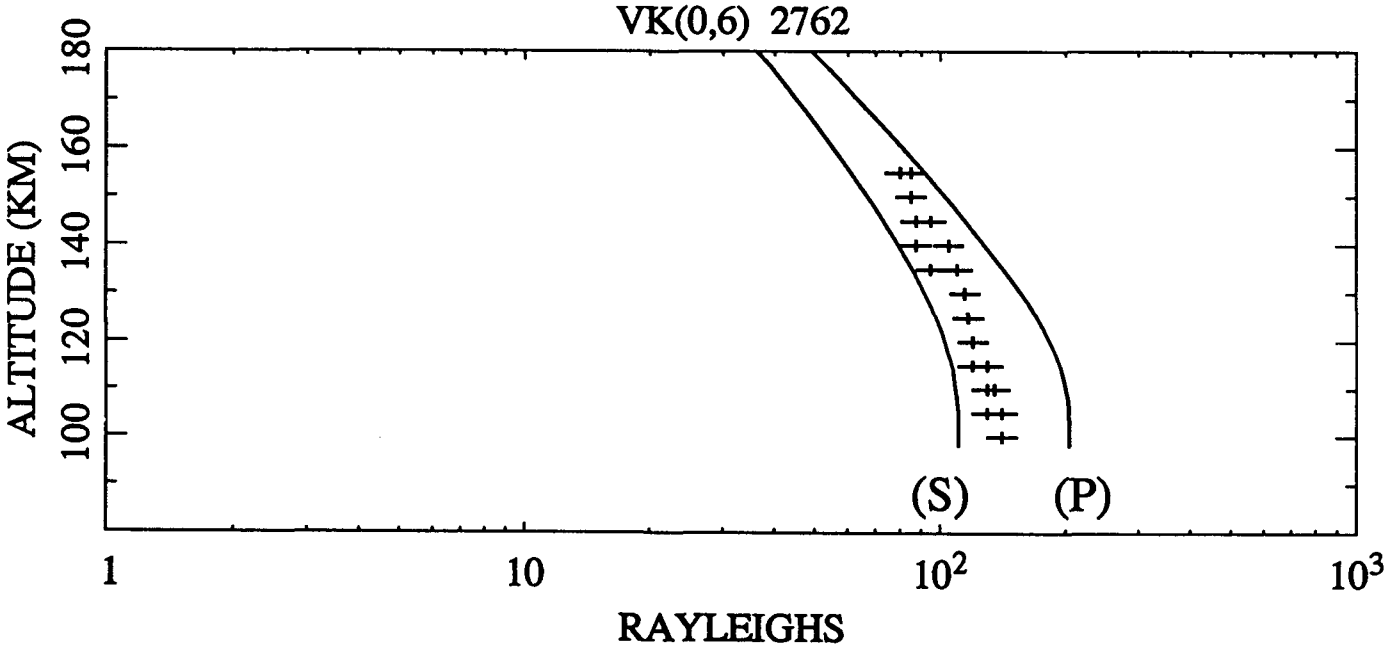

Figure 24

5. MODELING HIGH-LATITUDE F-REGION PATCHES

Our first efforts on this problem involved using time varying ionospheric convection to produce F-region patches in the winter polar cap. The time variation used was comparable to changes that result from changes in the B_y IMF. This effort led to a paper that was submitted to, accepted by, and published by Geophysical Research Letters.

Our next study, which has also led to a paper, focused on modeling daytime F layer patches over Sondrestrom. The purpose of the paper was to describe the details of our comprehensive, time-dependent, high-latitude, one-species, F-region model as well as to describe our initial attempts to model highly-structured plasma densities characterized by digisonde observations at Sondrestrom. The point of view that we took was that for the purposes of modeling, it is useful to classify the suggested mechanisms for producing patches into one of three types: 1) particle precipitation, 2) global **ExB** convection and 3) meso-scale **ExB** convection. Our conclusion was that on the particular day we modeled, both type 2 and type 3 mechanisms were playing a crucial role in structuring the ionospheric density. This paper was submitted to, accepted by, and published by Radio Science.

Most recently, we have been examining a scenario for producing density enhancements in the polar cap that was originally studied by *Anderson et al.* [1988]. Our purpose was to clarify what is happening in that scenario and verify that while it appears to be different from the scenarios described in *Sojka et al.* [1993] and *Decker et al.* [1994], in fact all three papers are describing essentially the same mechanism. That mechanism is one of changing in time the location of the type 3 trajectories. These are the trajectories where corotation and the magnetospheric potential act together to take plasma from the sunlit lower latitudes and bring it in and across the polar cap. In *Sojka et al.* [1993], the change was done by using the B_y dependence of the global convection pattern. In *Decker et al.* [1994], it was done by changing between Heelis patterns and Heppner/Maynard patterns. In repeating the Anderson et al. calculation, we have found that changing the polar cap radius and potential drop also changes where the type 3 trajectories are to be found. However, the change is not one of going from a pattern that has no type 3 trajectories and thus creates no tongue of ionization (TOI) to a pattern that does. Rather, both patterns have type 3 trajectories and create a TOI. What is different is that the large radius pattern creates a broader TOI as compared to that created by a small radius pattern. We also found that the signature on the ground is very sensitive to the chosen location. This indicates that under the same conditions, different high-latitude stations may have very different signatures of F-region structure. We are planning on exploring these differences by a series of simulations of various stations that were operating in the northern high latitudes during the IGY.

REFERENCES

Anderson, D.N., J. Buchau, and R.A. Heelis, Origin of Density Enhancements in the Winter Polar Cap Ionosphere, Radio Sci., 23, 513, 1988.

Creutzberg, F., R.L. Gattinger, F.R. Harris, S. Wozniak, and A. Vallance Jones, Auroral Studies with a Chain of Meridian Scanning Photometers 2. Mean Distributions of Proton and Electron Aurora as a Function of Magnetic Activity, J. Geophys. Res., 93, 14591, 1988.

Decker, D.T., C.E. Valladares, R. Sheehan, Su. Basu, D.N. Anderson, and R.A. Heelis, Modeling Daytime F Layer Patches Over Sondrestrom, Radio Sci., 29, 249, 1994.

Hardy, D.A., M.S. Gussenhoven, and D. Brautigam, A Statistical Model of Auroral Ion Precipitation, J. Geophys. Res., 94, 370, 1989.

Sojka, J.J., M.D. Bowline, R.W. Schunk, D.T. Decker, C.E. Valladares, R. Sheehan, D.N. Anderson, and R.A. Heelis, Modeling Polar Cap F Region Patches Using Time Varying Convection, Geophys. Res. Lett., 20, 1783, 1993.

PRESENTATIONS

We were involved in 16 presentations at various scientific meetings.

Jasperse, J.R., B. Basu, D.J. Strickland, R.E. Daniell, and D.T. Decker, "Combined Electron-Proton-Hydrogen Atom Aurora: Predictions of a Transport-Theoretical Model", presented at the Ionospheric Effects Symposium, May 4-6, 1993, Alexandria VA.

Abstract

In this paper, we present results for the first, self-consistent, transport-theoretic model for the combined electron-proton-hydrogen atom aurora. Using our model, we are able to study three auroral situations: a pure electron aurora; a pure proton-hydrogen atom aurora; and a combined electron-proton-hydrogen atom aurora. In comparing the pure electron to the pure proton-hydrogen atom aurora, we find that: (1) the secondary electron flux produced by the proton-hydrogen atom aurora is much softer than that produced by the electron aurora; (2) certain emission features (for example, 3371Å) are excited in completely different ways for the two aurora; and (3) the "eV per electron-ion pair" as a function of characteristic energy is nearly constant for the electron aurora and has a value of about 34, but varies significantly (~ 50%) for the proton-hydrogen atom aurora. For the combined aurora, we find that: (4) since the proton-hydrogen atom contribution to the total incident energy flux in the midnight sector is, on the average, about 20 to 25% of that of the electrons, when it is neglected the intensity of many emission features will also be underestimated, on the average, by about the same percentage; and (5) in the post midnight sector, a double bump in the altitude profiles of the E-region electron density is possible for certain auroral conditions.

Creamer, A.P., D.N. Anderson, P.H. Doherty, and B.G. Fejer, "Validation of the Phillips Lab Low Latitude Ionospheric Model with Jicamarca ISR Observations", presented at the Spring AGU Meeting, May 1993, Baltimore MD.

Abstract

We have used observed vertical ExB drift measurements from the incoherent scatter radar at Jicamarca, Peru (75° W, 11.6° N, 1° dip latitude) as an input to the Phillips Lab low latitude theoretical, time-dependent ionospheric model, and achieved excellent agreement with the observed peak parameters and electron density profiles for consecutive days in September and October, 1970. We extend our study to the solstices and to higher and lower solar activities where we have similar vertical drift and electron density measurements to reaffirm our results. We examine again our assumption that the vertical drift is the primary transport mechanism at the magnetic equator. We look also at the neutral winds which have a secondary effect on the peak of ionization during equinox, but become more important in determining the ionization during solstice periods. The low latitude model solves the ion continuity equation for plasma concentration through inputs of a neutral atmosphere, neutral winds, solar production, and loss rates. Typically, a model of the seasonal average vertical ExB drift is also included in the model. We use the actual ExB drift observed on the days for which we have electron density measurements as well as a specific climatological average drift as an input to the model. The climatological drifts are based on bimonthly vertical drift observations from Jicamarca as opposed to the traditional four month seasonal averages that most ExB drift models are based on. We find a marked improvement in the model calculations for Jicamarca when we use the actual drift as an input in our model, and demonstrate that we can realistically reproduce the ionization layer at the magnetic equator with knowledge of the vertical ExB drift.

Decker, D.T., "Modeling the LTCS 2 and 6 Periods with the Phillips Laboratory Ionospheric Model", presented at the PRIMO Workshop, CEDAR Meeting, Boulder CO, June 1993.

Decker, D.T., "Modeling Polar Cap Patches: The Present Status", presented at the HLPS Workshop, CEDAR Meeting, Boulder CO, June 1993.

Decker, D.T., J.R. Jasperse, B. Basu, and D.J. Strickland, "The Theory of the Electron-Proton-Hydrogen Atom Aurora: Comparison with Observations", presented at the NATO Advance Research Workshop 20 Annual European Meeting on Atmospheric Studies by Optical Methods, September 1993, Apatity, Russia.

Abstract

Recently, a self-consistent theory for the combined electron-proton-hydrogen atom aurora has been developed. To date, the portions of the model involving just electron transport have been tested with good agreement against a variety of data. Comparisons between the proton-hydrogen atom portion of the model and data are just beginning. In this paper, we review our initial attempts to validate this fully coupled three component auroral model with particular emphasis on the role of the protons and hydrogen atoms.

Specifically, we model three separate auroras and compare with different types of observations. In case 1, we model upgoing electrons observed by the DE-2 satellite as it passes through a region of downgoing protons and electrons. Our second case involves modeling the E region electron density observed by the Chatanika radar during a proton aurora. For our third case, we model the column emission rates observed during a combined aurora by rocket borne photometers. In all three cases, these initial attempts to test the theory versus data are judged to be successful.

Klobuchar, J.A., S. Basu, and P.H. Doherty, "Potential Limitations in Making Absolute Ionospheric Measurements Using Dual Frequency Radio Waves from GPS Satellites", presented at the Ionospheric Effects Symposium, May 4-6, 1993, Alexandria VA.

Abstract

Ionospheric workers who monitor L-band radio transmissions from Global Positioning Systems (GPS) satellites can encounter misleading results in measuring various transionospheric parameters. This paper discusses sources of potential errors in determining absolute Total Electron Content (TEC), and in obtaining accurate values of amplitude scintillation index, S_4, from radio waves from GPS satellites.

Decker, D.T., C.E. Valladares, R. Sheehan, Su. Basu, D.N. Anderson, and R.A. Heelis, "Modeling Daytime F Layer Patches Over Sondrestrom", presented at the Fall AGU meeting, December 1993, San Francisco CA.

Abstract

A comprehensive time-dependent, high-latitude, one-species F-region model has been developed to study the various physical processes which are believed to affect the polar cap plasma density distributions as a function of altitude, latitude, longitude, and local time. These processes include production of ionization by solar extreme ultraviolet radiation and particle precipitation; loss through charge exchange with N2 and 02; and transport by diffusion, neutral winds, and convection E X B drifts. For this paper, we have modeled highly-structured plasma densities characterized by digisonde observations at Sondrestrom using both a time-dependent global convection pattern and spatially localized regions of transient high-speed flow. We find that the model is very sensitive to the details of the time-dependent convection pattern, and both the time dependence and the high-speed flows contribute to the F-region structure. Further, when we use high-speed flows based on radar observations from a specific day, the simulated density structure is in reasonable agreement with that day's digisonde observations.

Valladares, C.E., D.T. Decker, R. Sheehan, Su. Basu, and D.N. Anderson, "Observations and Workstation Modeling of Large Scale Plasma Density Structures in the Cusp/Cleft Region", presented at the Fall AGU meeting, December 1993, San Francisco CA.

Abstract

During the maximum phase of the solar cycle, several experimental campaigns were conducted at high latitudes to investigate the formation, transit, and ultimate fate of polar cap patches. Here we report several observations of the formation of large-scale (100's of km) plasma structures in the cusp/cleft region. On one occasion, the Sondrestrom incoherent scatter radar clearly identified the formation of a patch-like structure and followed its entry into the polar cap. The event started with the appearance of a fast plasma jet containing velocities in excess of 2 km s^{-1}. This plasma jet consisted of a channel extending 300 km in width, where the F-region ion temperature reached 4000 K. It is suggested that the recombination loss of O^+ increased by a factor > 10 producing a trench of low density in between regions of higher Ne. This event has been modeled using a time-dependent one-species F-region model of the high latitude ionosphere. Our model includes a spatially localized region of transient high-speed flows located adjacent and poleward of a region containing typical cusp precipitation. To properly compare the modeled and the measured data, we have conducted elevation scans through the simulated volume mimicking the radar scans. We find that the simulated plasma density in the jet region is in good agreement with the experimental data. We have also varied the total and the average energy of the electrons deposited in the cusp region in accordance with values measured by low altitude satellites. The results of this simulation will be reported in this paper.

Snow, R.W., A.W. Osborne, J.A. Klobuchar, and P.H. Doherty, "Ionospheric Corrections to Precise Time Transfer Using GPS", presented at the Precise Time Transfer Institute meeting, December 6-9, 1993, Marina Del Ray CA.

Abstract

The free electrons in the earth's ionosphere can retard the time of reception of GPS signals received at a ground station, compared to their time in free space, by many tens of nanoseconds, thus limiting the accuracy of time transfer by GPS. The amount of the ionospheric time delay is proportional to the total number of electrons encountered by the wave on its path from each GPS satellite to a receiver. This integrated number of electrons is called Total Electron Content, or TEC. Dual frequency GPS receivers designed by Allen Osborne Associates Inc. (AOA) directly measure both the ionospheric differential group delay and the differential carrier phase advance for the two GPS frequencies, and derive from this the TEC between the receiver and each GPS satellite in track. The group delay information is mainly used to provide an absolute calibration to the relative differential carrier phase, which is an extremely precise measure of relative TEC. The AOA Mini Rogue ICS-4Z receiver and the Turbo-Rogue ICS-4000Z receivers normally operate using the GPS-P code, when available, and switch to cross correlation signal processing when the GPS satellites are in the Anti-Spoofing (A/S) mode and the P-code is encrypted.

An AOA ICS-4Z receiver has been operated continuously for over a year at Hanscom AFB MA to determine the statistics of the variability of the TEC parameter using signals from up to four different directions simultaneously. The four channel ICS-4Z and the eight channel ICS-4000Z have proven capabilities to make precise, well-calibrated, measurements of the ionosphere in several directions simultaneously. In addition to providing ionospheric corrections for precise time transfer via satellite, this dual frequency design allows full code and automatic codeless operation of both the differential group delay and differential carrier phase for numerous ionospheric experiments being conducted. Statistical results for the initial year of ionospheric time delay data collected in the northeastern United States using the ICS-4Z ionospheric calibration system, and initial results with the ICS-40OOZ, will be presented.

Doherty, P.H., B. Fejer, D.N. Anderson, and A.P. Creamer, "Low Latitude Ionospheric Response to Jicamarca, Storm-Time Vertical Drift Measurements", presented at the Cedar Storm Study workshop, March 1993, Millstone Hill, Westford MA, and the Spring AGU Meeting, May 1993, Baltimore MD.

Abstract

Observed vertical drift velocities measured by the Jicamarca, Peru incoherent scatter radar facility during June 13-14, 1991 geomagnetic storm are incorporated into the time-dependent, theoretical plasma continuity equation to calculate electron density profiles as a function of latitude and local time. The ionospheric response to these storm-time drifts are compared with the quiet-time ionosphere resulting from quiet-time vertical drifts measured at Jicamarca. In addition, the drifts measured during the June 13-14, 1991 storm are compared to the drifts measured during the March 22-23, 1990 geomagnetic storm, and the resulting ionospheric profiles are compared with each other and with the quiet-time profiles. It is found that for the March 22-23 storm, the strong enhancement in vertical ExB drift after 1800 LT causes calculated Hmax values to exceed 900 km at 2100 LT. Comparisons are made with DMSP in-situ electron densities at 850 km altitudes.

Klobuchar, J.A., P. Doherty, and M. El-Arini, "Potential Ionospheric Limitations to Wide Area Differential GPS", presented at ION-GPS 1993, September 21-24, 1993, Salt Lake City UT.

Abstract

Navigation and positioning using wide area differential GPS potentially suffers from the unknown spatial variability of ionospheric range errors between locations where dual frequency measurements from GPS satellites are being made. In the CONUS region, it is possible to correct for most of the ionospheric range error by using a sufficient number of dual frequency GPS codeless receivers to specify the variability of the ionosphere over the entire region. Over the large expanse of the North Atlantic Ocean region, for instance, where it is not possible to continuously measure the ionospheric range error except for a few locations around the ocean circumference, large errors in ionospheric time delay will occasionally limit the overall wide area DGPS positioning accuracy.

Using ionospheric data collected from a number of stations in the United States and Europe over the last solar cycle, the statistics of differences in range error over station separations from approximately 200 km to over 4000 km are presented. During periods of high magnetic activity, the correlation distance is small, but these events are infrequent. For the mid-latitudes, the goal is to keep ionospheric range error below one meter 95% of the time. This goal is attainable during solar minimum conditions, but not during periods of very high solar activity.

Jasperse, J.R., B. Basu, D.J. Strickland, D.T. Decker, J.R. Sharber, and J.D. Winningham, "Theory of the Electron-Proton-Hydrogen Atom Aurora: Comparison With Observations", presented at the Fall AGU meeting, December 1993, San Francisco CA.

Abstract

Recently, the first self-consistent theory for the combined electron-proton-hydrogen atom aurora has been developed. To date, the portions of the model involving just electron transport have been tested against a variety of data with good agreement. Comparisons between the proton-hydrogen atom portion of the model and experiment are just beginning. In this paper, we review the initial attempts to validate this fully coupled three component auroral model with particular emphasis on the role of the protons and hydrogen atoms.

In particular, the major outputs of the model are the differential fluxes of the energetic particles, the resulting vertical ion density profile, and selected emission features. We will present comparisons of these quantities with measurements from satellites, rockets, and ground-based instruments.

El-Arini, M.B., J.A. Klobuchar, and P.H. Doherty, "Evaluation of the Wide-Area Differential GPS (WDGPS) Ionospheric Grid Algorithm During the Peak of the Current Solar Cycle", presented at the National Technical Meeting of the Institute of Navigation, January 24-26, 1994, San Diego CA.

Abstract

The Federal Aviation Administration (FAA) Satellite Program Office, ARD-70, is developing a Wide Area GPS Augmentation (WGA) system to achieve Category 1 (CAT1) or near CAT1 precision landing horizontal and vertical requirements. The ionospheric corrections are based on the WADGPS ionospheric grid algorithm which was developed previously by MITRE/CAASD and the Air Force Phillips Laboratory (AFPL). Without considering ground station redundancy, we suggested 15 remote reference stations including one master station to support a proposed CONUS ionospheric grid. The summary of this algorithm is as follows: a) each reference station measures the ionospheric delay for each visible satellite (mask angle greater than or equal to 5 degrees) using a dual-frequency GPS receiver and sends this information (in real time) to the master station, b) the master station collects all ionospheric data from all reference stations and estimates the vertical ionospheric delay for each node of an imaginary fixed grid (every 10 degrees in latitude and longitude) on the ionospheric sphere (350 km above the Earth's surface), c) the master station sends the vertical delay estimate of each node of the grid as well as the node latitude and longitude (or an identification number) to all user receivers via an Inmarsat satellite (or any other communication satellite), and d) the user receiver computes the latitude and longitude of its pierce points (one pierce point per visible satellite). For each pierce point, the receiver computes its slant ionospheric delay.

We tested this algorithm using measured data during 1992 and 1993 from three remote reference stations 500 miles from the user on the east coast of the United States. The prediction of the slant ionospheric delay is compared with a measured dual-frequency slant ionospheric range delay at the user location. The prediction slant range error was within 4m (95th percentile).

The purpose of this paper is to evaluate the grid algorithm using measured data during January and February 1991 which is very close to the peak of the current solar cycle. The data were collected by the Jet Propulsion Laboratory (JPL) using a network of dual-frequency receivers. The correlation distance is also calculated.

Decker, D.T., D.N. Anderson, and B.W. Reinisch, "Day to Day Comparison of Calculated and Observed Electron Density Profiles at Midlatitudes" presented at Spring AGU meeting, May 1993, Baltimore MD, and the XXIVth General Assembly of the International Union of Radio Science, August 1993, Kyoto, Japan.

Abstract

Over the last several years, there has been an increasing effort to validate various theoretical models of the earth's ionosphere. In the work done to date, the focus has been almost exclusively on comparisons between a calculation of a 24-hour day using typical or average inputs with either monthly means of observations or data from a "typical" quiet day. Thus, what is being evaluated is our ability to model climatology. But, on the other hand, there is growing interest on how well the day-to-day "weather" of the ionosphere can be modeled. With that in mind, we are simulating the day-to-day variations for several months at various midlatitude stations.

Our first goal is to simply see how well a theoretical model simulates the ionospheric day-to-day variability when that model is essentially driven by statistical inputs. From such a study, we hope to develop a better understanding of which days of data should be used for climatology studies. A second goal is to study under what geophysical conditions, if any, might we model the day-to-day variability in terms of variations in the neutral wind. Our approach is to do four sets of simulations using four different sources for the neutral winds. The first source is the empirical model HWM90 based on satellite and ground-based observations of the thermospheric winds. For our second source, we use the VSH (Vector Spherical Harmonic) Model based on runs of a general circulation model of the thermosphere and ionosphere (the NCAR-TIGCM). In our third set of simulations, we use winds derived from the F2 peak heights contained in the IRI (International Reference Ionosphere). Finally, in the fourth set of simulations, we use a "real-time" input by using the observed F2 peak heights to derive effective winds.

JOURNAL ARTICLES

Sojka, J.J., M.D. Bowline, R.W. Schunk, D.T. Decker, C.E. Valladares, R. Sheehan, D.N. Anderson, and R.A. Heelis, Modeling polar cap F region patches using time varying convection, Geophys. Res. Lett., 20, 1783, 1993.

Abstract

Creation of polar cap *F*-region patches are simulated for the first time using two independent physical models of the high latitude ionosphere. The patch formation is achieved by temporally varying the magnetospheric electric field (ionospheric convection) input to the models. The imposed convection variations are comparable to changes in the convection that result from changes in the B_y IMF component for southward interplanetary magnetic field (IMF). Solar maximum-winter simulations show that simple changes in the convection pattern lead to significant changes in the polar cap plasma structuring. Specifically, in winter, as enhanced dayside plasma convects into the polar cap to form the classic tongue-of-ionization (TOI) the convection changes produce density structures that are indistinguishable from the observed patches.

Decker, D.T., C.E. Valladares, R. Sheehan, Su. Basu, D.N. Anderson, and R.A. Heelis, Modeling daytime F layer patches over Sondrestrom, Radio Sci., 29, 249, 1994.

Abstract

A comprehensive, time-dependent, high-latitude, one-species *F* region model has been developed to study the various physical processes which are believed to affect the polar cap plasma density distributions as a function of altitude, latitude, longitude, and local time. These processes include production of ionization by solar extreme ultraviolet radiation and particle precipitation; loss through charge exchange with N_2 and O_2; and transport by diffusion, neutral winds, and convection $\mathbf{E} \times \mathbf{B}$ drifts. In our initial calculations we have modeled highly structured plasma densities characterized by digisonde observations at Sondrestrom using both a time-dependent global convection pattern and spatially localized regions of transient high-speed flow. We find that the model is very sensitive to the details of the time-dependent convection pattern, and both the time dependence and the high-speed flows contribute to the *F*-region structure. Further, when we use high-speed flows based on specific radar observations the simulated density structure is in reasonable agreement with that day's digisonde observations.

Jasperse, J.R., B. Basu, J.M. Retterer, D.T. Decker, and T. Chang, "High Frequency Electrostatic Plasma Instabilities and Turbulence Layers in the Lower Ionosphere", accepted for publication in Journal of Geophysical Research.

Abstract

It has been known for some time that calculations of the collisional electron distribution function in the 2 to 5 eV energy range which neglect wave-particle interactions disagree with rocket measurements in both the auroral and sunlit, midlatitude ionospheres. The latter show a filling-in of the 2 to 5 eV valley in the isotropic distribution function predicted by the zero-order calculations. Several narrow layers (each about 4 to 10 km thick) of intense electron heating from 98 to 130 km and a broad layer of weaker electron heating from about 135 to 210 km in the sunlit, midlatitude ionosphere have also been observed. More recently, a rocket experiment in the auroral zone recorded intense plasma waves near the upper hybrid frequency in the altitude range of 130 to 170 km. We can tie these observations together by invoking the existence of the electron cyclotron and upper hybrid plasma instabilities described by Basu et al. [1981, 1982]. The free energy source for these instabilities is the suprathermal, shell-like bump in the electron energy distribution near 5 eV. In this paper, we review and extend the linear collisional stability analysis. We also present a new collisional quasilinear analysis and particle-in-cell plasma simulations which we have carried out in our study of this problem.

Preble, A.J., D.N. Anderson, B.G. Fejer, and P.H. Doherty, "Comparison Between Calculated and Observed F-Region Electron Density Profiles at Jicamarca, Peru," accepted for publication in Radio Science.

Abstract

Electron density profiles and isodensity contours derived from Jicamarca Incoherent Scatter Radar observations in Peru for 1 to 2 October, 1970 are compared in detail with results from the Phillips Laboratory Ionospheric Model (PLIM). This model solves the ion continuity equation for O^+ concentration through production, loss, and transport of ionization. The primary factor controlling the peak plasma density at Jicamarca is the vertical **ExB** drift which drives the ionization upward during the day and downward at night. When we use the measured drift in the model, we achieve excellent results with the measured electron density profiles. We illustrate the sensitivity of the low latitude plasma density calculations to changes in the vertical **ExB** drift and changes in the neutral winds. We also compare the calculated profile and peak parameters with an empirical model - the International Reference Ionosphere (IRI). We illustrate several limitations associated with the IRI which contribute to its limited capability at the magnetic equator.